ESC European Society of Cardiology

Cardiovascular Research (2023) **120**, 188–202
https://doi.org/10.1093/cvr/cvad126

# Activation of endothelial TRPM2 exacerbates blood–brain barrier degradation in ischemic stroke

**Pengyu Zong[1,2], Jianlin Feng[1], Cindy X. Li[1], Evan R. Jellison[3], Zhichao Yue[1], Barbara Miller[4], and Lixia Yue [1,2]***

[1]Department of Cell Biology, Calhoun Cardiology Center, University of Connecticut School of Medicine (UConn Health), 263 Farmington Ave, Farmington, CT 06030, USA; [2]Department of Neuroscience, University of Connecticut School of Medicine (UConn Health),263 Farmington Ave, Farmington, CT 06030, USA; [3]Department of Immunology, University of Connecticut School of Medicine (UConn Health), 263 Farmington Ave, Farmington, CT 06030, USA; and [4]Department of Biochemistry and Molecular Biology, The Pennsylvania State University College of Medicine, 500 University Drive, Hershey, PA 17033, USA

*Received 30 September 2022; revised 23 March 2023; accepted 23 May 2023; online publish-ahead-of-print 18 August 2023*

**Time of primary review: 56 days**

**Aims**

Damage of the blood–brain barrier (BBB) is a hallmark of brain injury during the early stages of ischemic stroke. The subsequent endothelial hyperpermeability drives the initial pathological changes and aggravates neuronal death. Transient receptor potential melastatin 2 (TRPM2) is a $Ca^{2+}$-permeable nonselective cation channel activated by oxidative stress. However, whether TRPM2 is involved in BBB degradation during ischemic stroke remains unknown. We aimed to investigate the role of TRPM2 in BBB degradation during ischemic stroke and the underlying molecular mechanisms.

**Methods and results**

Specific deletion of *Trpm2* in endothelial cells using *Cdh5 Cre* produces a potent protective effect against brain injury in mice subjected to middle cerebral artery occlusion (MCAO), which is characterized by reduced infarction size, mitigated plasma extravasation, suppressed immune cell invasion, and inhibited oxidative stress. *In vitro* experiments using cultured cerebral endothelial cells (CECs) demonstrated that either *Trpm2* deletion or inhibition of TRPM2 activation attenuates oxidative stress, $Ca^{2+}$ overload, and endothelial hyperpermeability induced by oxygen–glucose deprivation (OGD) and CD36 ligand thrombospondin-1 (TSP1). In transfected HEK293T cells, OGD and TSP1 activate TRPM2 in a CD36-dependent manner. Noticeably, in cultured CECs, deleting *Trpm2* or inhibiting TRPM2 activation also suppresses the activation of CD36 and cellular dysfunction induced by OGD or TSP1.

**Conclusions**

In conclusion, our data reveal a novel molecular mechanism in which TRPM2 and CD36 promote the activation of each other, which exacerbates endothelial dysfunction during ischemic stroke. Our study suggests that TRPM2 in endothelial cells is a promising target for developing more effective and safer therapies for ischemic stroke.

* Corresponding author. Tel: +860-679-3869; fax: 860-679-1426, Email: lyue@uchc.edu

## Graphical Abstract

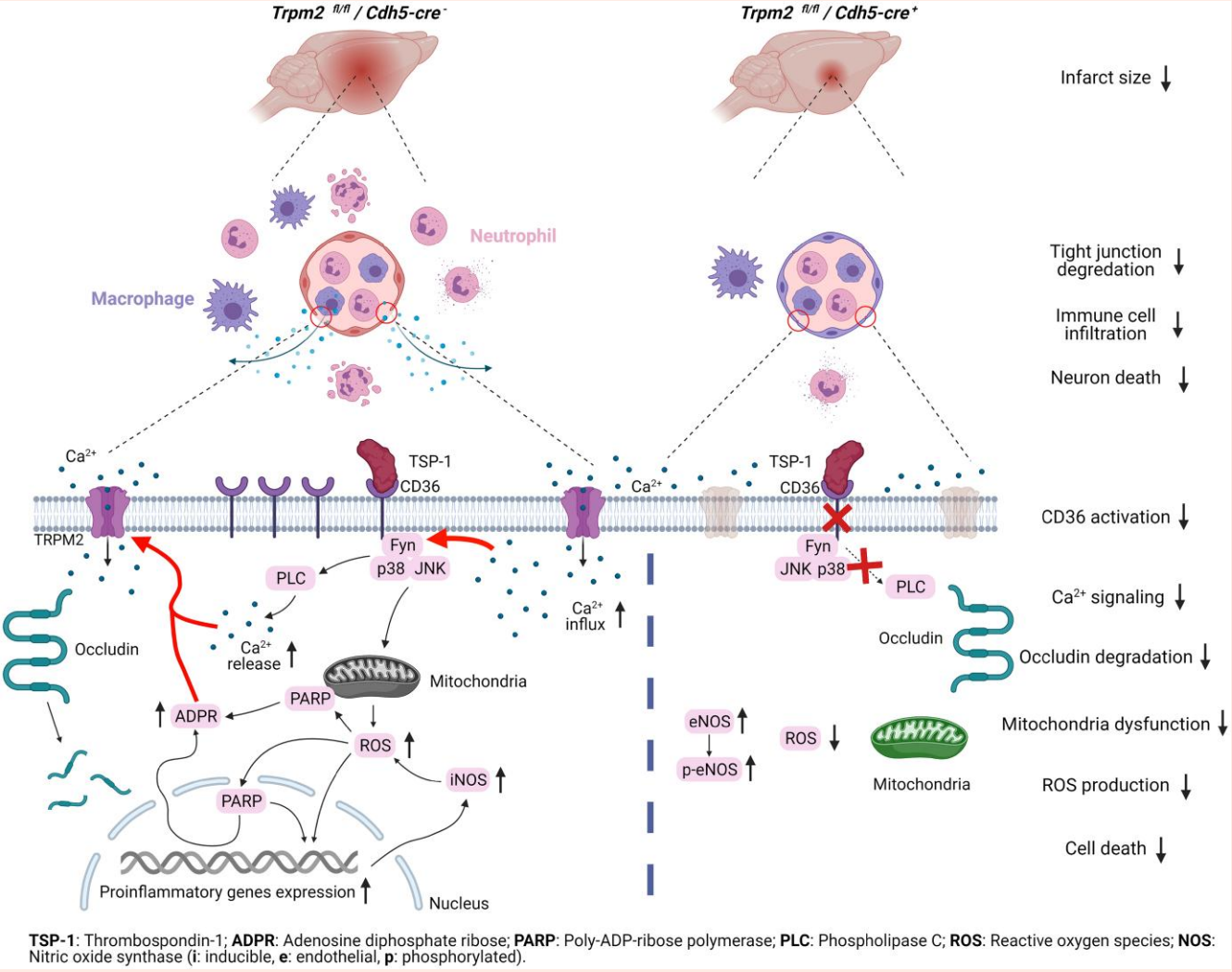


TRPM2-mediated $Ca^{2+}$ signaling is essential for CD36-induced endothelial dysfunction and tight junction degradation. The activation of CD36 and TRPM2 forms a positive feedback loop that promotes blood–brain barrier degradation during ischemic stroke.

**Keywords** Transient receptor potential melastatin 2 (TRPM2) • Ischemic stroke • Blood–brain barrier (BBB) • Thrombospondin-1 (TSP1) • CD36 • Endothelial hyperpermeability

# 1. Introduction

Ischemic stroke is a major health issue worldwide, with over 10 million new cases happening every year.[1] The central pathological feature of ischemic stroke is neuronal death.[2] Unfortunately, drugs mitigating neuronal death, such as *N*-methyl-D-aspartate (NMDA) receptor antagonists, ion channel blockers, caspase inhibitors, and neurotrophic factors, all failed to show protective effects in patients with ischemic stroke.[3,4] The failure of directly targeting neurons in the treatment of ischemic stroke patients has led to the consensus that targeting non-neuron cells, which contribute to neuronal death during ischemic stroke, may provide better therapeutic outcome.[5,6] Given the complexity of ischemic stroke, all the cells distal to the occlusion site, such as endothelial cells in the neurovascular unit (NVU), are influenced and involved in the progression of ischemic brain injury.

NVU is composed of endothelial cells, pericytes, basal lamina, smooth muscle cells, surrounding astrocytes, and neurons.[7] Anatomically, endothelial cells are the core component of NVU.[8] Compared to peripheral endothelial cells, a prominent feature of cerebral endothelial cells (CECs) are the widely linked tight junctions,[9] which are critical for the formation of the blood–brain barrier (BBB). During ischemic stroke, tight junctions between endothelial cells are disrupted, and BBB is degenerated, which leads to fluid imbalance and immune cell invasion into the brain.[10–12] Both cerebral edema and inflammatory infiltration aggravate neuronal death and increase the mortality of patients with ischemic stroke.[11,13] Therefore, preserving BBB integrity by mitigating endothelial dysfunction should protect the brain against ischemic stroke. However, the molecular mechanisms causing endothelial dysfunction during ischemic stroke are poorly understood.[14]

CD36 in endothelial cells has been found to be involved in endothelial dysfunction during ischemic stroke.[15] Interestingly, recent single-cell RNA sequencing works have identified a distinct endothelial cell population with abundant CD36 expression.[16] CD36 is a member of the class B

scavenger receptor family. This membrane protein has a large extracellular domain, which binds to different ligands, such as oxidized low-density lipoprotein (ox-LDL), thrombospondins (TSPs), and fibrillar β amyloid (fAβ).[17] Ligand binding to CD36 triggers downstream signaling cascades, including activation of Fyn, JNK, and p38, all of which result in oxidative stress and cellular dysfunction in a variety of pathological conditions, including Alzheimer's disease and ischemic stroke.[18–21] However, the underlying mechanisms regulating the activation of CD36 signaling remain unclear.[15]

TRPM2 is an oxidative stress sensitive and $Ca^{2+}$-permeable nonselective cation channel activated by intracellular $Ca^{2+}$ and ADP-ribose (ADPR). ADPR can be generated during oxidative stress and promotes cellular damage by activating TRPM2.[22] TRPM2 is ubiquitously expressed in various cell types including endothelial cells and macrophages and is most abundantly expressed in the central nervous system.[23] Global *Trpm2* knockout in mice has been shown to alleviate ischemic stroke, but the mechanisms underlying this phenomenon are not fully understood.[24–26] Knockdown or inhibition of TRPM2 attenuates the enhanced endothelial permeability induced by $H_2O_2$ in isolated pulmonary artery endothelial cells *in vitro*,[24] and *Trpm2* deletion in endothelial cells reduced neutrophil transmigration in the lung in response to lipopolysaccharide (LPS) challenge.[27] However, it is unknown whether TRPM2 in CECs influences endothelial permeability during ischemic stroke. As mentioned earlier, endothelial cells in the central nervous system are significantly different from peripheral endothelial cells. Thus, we propose that TRPM2 promotes endothelial dysfunction and BBB degradation in ischemic stroke.

In this study, we found that selective deletion of *Trpm2* in endothelial cells protects mice against ischemic stroke. *Trpm2* deletion inhibits oxidative stress and prevents tight junction degradation between CECs and reduces the infiltration of immune cells into the brain after ischemic stroke. Mechanistically, we revealed that TRPM2 can be activated by CD36 ligand TSP1. Moreover, TRPM2 is required for the activation of CD36 signaling cascades in CECs induced by oxygen–glucose depletion (OGD) or TSP1. Our results establish an inter-dependent regulation of TRPM2 and CD36 in causing endothelial hyperpermeability during ischemic stroke, suggesting that targeting TRPM2 in CECs may represent a more effective approach to mitigate ischemic brain injury.

# 2. Methods

Animal experiments were approved by the animal care committees of University of Connecticut School of Medicine. All experimental procedures and protocols were approved by the Institutional Animal Care and Use Committee (IACUC) of University of Connecticut School of Medicine (animal protocol: AP-200135-0723) and were conducted in accordance with the US National Institutes of Health Guidelines for the Care and Use of Laboratory Animals. Mice were euthanized based on IACUC-approved protocols.

For details on materials regarding the origin of animals, plasmids, and antibodies used in our study, please see the Supplementary material online. Furthermore, detailed information regarding surgery procedures, cell cultures, plasmid transfections, whole-cell current recordings, immunoblot analysis, immunofluorescence staining, and $Ca^{2+}$ and mitochondrial imaging techniques can also be found in the Supplementary material online.

# 3. Results

## 3.1 Endothelial cell–specific *Trpm2* deletion attenuates ischemic stroke

To examine the role of endothelial TRPM2 in ischemic stroke, *Trpm2* was selectively knocked out in endothelial cells using *Cdh5-cre* mice (see Supplementary material online, *Figure S1A*), which wasconfirmed by western blot (WB) (see Supplementary material online, *Figure S1B and C*) and whole-cell current recording (see Supplementary material online, *Figure S1D and E*). Importantly, TRPM2 knockout did not influence the expression of other oxidative stress-related TRP channels, TRPV1, TRPA1, TRPM4, TRPM7, and TRPM8, in endothelial cells (see Supplementary material online, *Figure S1F*). The endothelial cell–specific *Trpm2* knockout ($Cre^+$, $Trpm2^{fl/fl}$) mice are designated as eM2KO, while the $Cre^-$ littermates ($Cre^-$, $Trpm2^{fl/fl}$) are designated as WT hereafter.

Infarct volume was examined by 2,3,5-triphenyltetrazolium chloride (TTC) staining 24 h after MCAO (*Figure 1A*). The successful occlusion of middle cerebral artery was confirmed by reduced blood flow during occlusion measured by laser Doppler blood FlowMeter (*Figure 1B*; Supplementary material online, *Figure S1G*). Mice with *Trpm2* deletion in endothelial cells (eM2KO) exhibited smaller infarction size ($18.9 \pm 1.4\%$ in eM2KO vs. $34.4 \pm 3.5\%$ in WT) and improved neurological performance ($1.4 \pm 0.2$ in eM2KO vs. $2.6 \pm 0.3$ in WT) (*Figure 1A*, *C*, and *D*). Increase of plasma extravasation examined by Evans blue assay (*Figure 1E* and *F*) after MCAO was attenuated in eM2KO mice ($0.3 \pm 0.1$ in eM2KO vs. $0.7 \pm 0.1$ in WT).

We also evaluated the early protective effects of eM2KO after ischemic stroke. We found that eM2KO reduced brain infarction as well as Evans blue leakage as early as 6 h after MCAO (*Figure 1G–I*) and prevented the compromise of neurobehavior functions (*Figure 1J*).To examine whether eM2KO produces a long-term protective effect against ischemic stroke, we performed TTC staining and Evans blue assay 7 days after the reperfusion of MCAO and observed reduced brain infarction and BBB leakage in eM2KO group (*Figure 1K–M*). Moreover, we evaluated the brain function at Days 1, 3, and 7 by neurological deficit (ND) score and rotarod assay. We found that eM2KO prevented the deterioration of neurological performance after MCAO (*Figure 1N*; Supplementary material online, *Figure S1H*). These results indicate that endothelial cell–specific TRPM2 knockout attenuates ischemic stroke in mice.

Ischemic stroke in human patients usually involves multiple risk factors, including hypercholesterolemia.[28] We sought to understand whether eM2KO still produces a protective effect in model mice with at least one risk factor. We fed mice with high-fat diet (HFD) to induce hypercholesterolemia. After a 4-month HFD treatment, all mice developed obesity and dyslipidemia, and there is no difference in the body weight (see Supplementary material online, *Figure S1I*) and serum cholesterol level (see Supplementary material online, *Figure S1J*) between WT and eM2KO mice. We found that after MCAO, eM2KO mice still exhibited smaller infarct size (see Supplementary material online, *Figure S1K and L*) and preserved neurobehavior performance (see Supplementary material online, *Figure S1M*). These data further confirm the potential translational values of our findings in human patients.

TRPM2 was previously shown to promote angiogenesis in a hindlimb ischemia model.[29] Thus, we examined whether eM2KO influence vasculature and cerebral blood flow (CBF). We used laser speckle imaging system to monitor the real-time *in vivo* cerebral circulation.[30] We found that eM2KO did not cause a significant change in vessel diameter (*Figure 1O* and *P*) or CBF (*Figure 1Q* and *R*). Moreover, there was no difference of the endothelial cell density (*Figure 1S* and *T*) and capillary diameter/density between WT and eM2KO mice, suggesting that TRPM2 knockout does not affect the basal cerebral microcirculation (*Figure 1U–W*). Our data indicate that TRPM2 does not influence the vasculature development in the brain under normal physiological conditions.

Endothelial cells are the core component of the NVU/BBB, and the loss of tight junctions between endothelial cells is one of the hallmark events at the initial stage of ischemic stroke.[14] As occludin is a crucial component of the tight junction,[31] we investigated whether occludin function was impacted. After MCAO, the expression of occludin was decreased in WT mice, whereas this decrease was inhibited in eM2KO mice (see Supplementary material online, *Figure S2A and B*). Also, TUNEL staining revealed that the apoptosis of endothelial cells after MCAO was attenuated by eM2KO (see Supplementary material online, *Figure S2C and D*).

## 3.2 eM2KO alleviates post-stroke inflammatory infiltration

Immune cell infiltration follows BBB degradation and aggravates brain injury. We prepared single-cell suspension of the brain following a well-

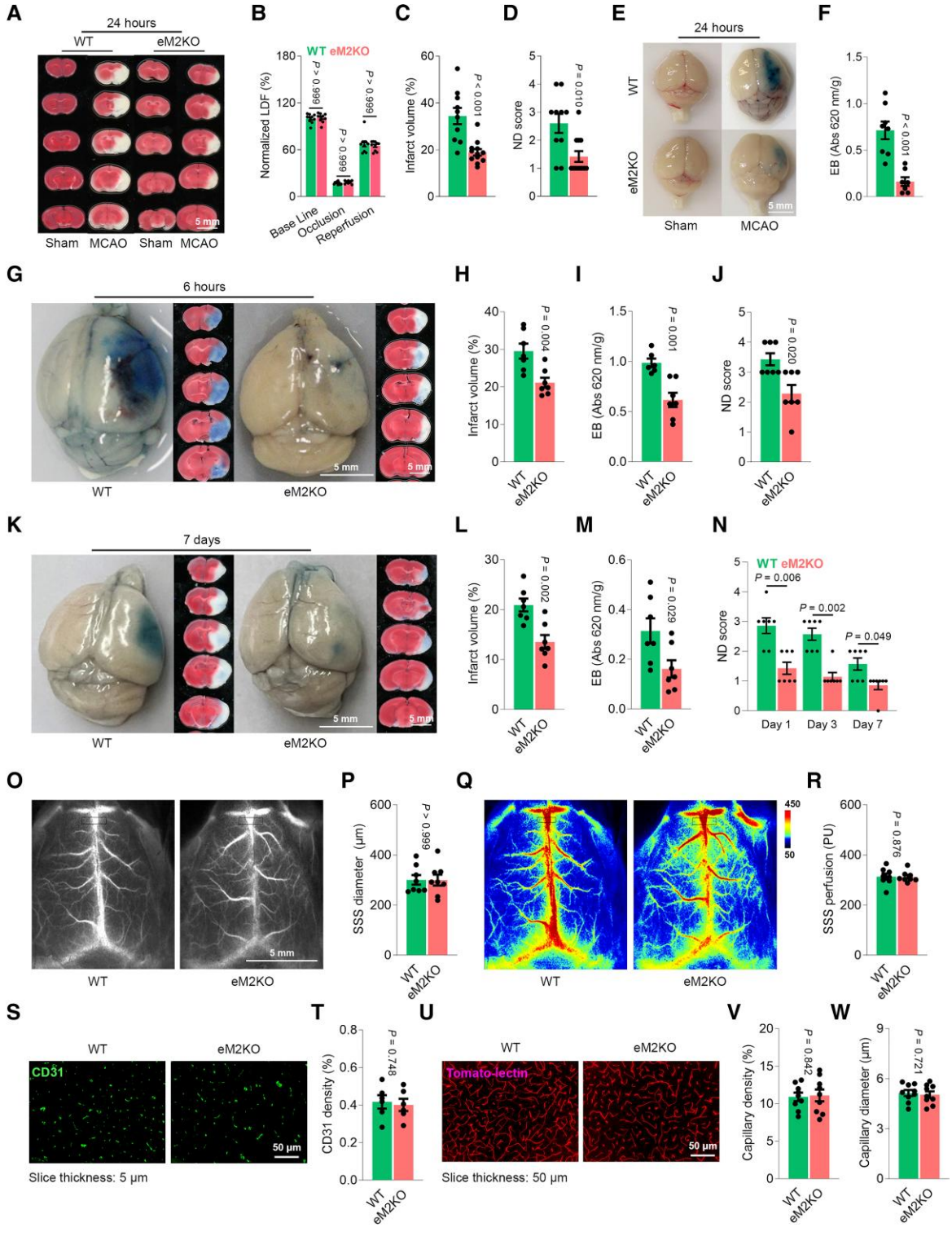


**Figure 1** Endothelial cell–specific *Trpm2* deletion alleviates ischemic stroke. (*A–F*) Evaluation 24 h after MCAO. (*A*) TTC staining of brain slices (1 mm). (*B*) Blood flow changes. Reduction of CBF for over 85% indicates successful MCAO. (*C*, *D*) Mean infarct volume and average ND score after MCAO from WT ($n = 10$) and eM2KO mice ($n = 12$). (*E*) Evans blue assay of whole brain. (*F*) Mean Evans blue absorption at 620 nm after MCAO from WT ($n = 8$) and eM2KO mice ($n = 8$). (*G–J*) Evaluation 6 h after MCAO ($n = 6, 7$). (*G*) Evans blue assay and TTC staining. (*H*) Mean infarct volume. (*I*) Mean Evans blue absorption. (*J*) Average ND score. (*K–N*) Evaluation 7 days after MCAO ($n = 7, 7$). (*K*) Evans blue assay and TTC staining. (*L*) Mean infarct volume. (*M*) Quantification of Evans blue assay. (*N*) Average ND score. (*O*) Representative images of cerebral vasculature imaging. (*P*) Quantification of superior sagittal sinus (SSS) diameter ($n = 8, 9$). (*Q*) Representative images of cerebral perfusion. (*R*) Quantification of SSS perfusion ($n = 8, 9$). (*S*) Representative images of CD31 staining of brain slices (5 μm). (*T*) Quantification of CD31 density ($n = 6, 6$). (*U*) Representative images of tomato lectin microvasculature staining of brain slices (50 μm). (*V*) Quantification of capillary density ($n = 8, 9$). (*W*) Quantification of capillary diameter ($n = 8, 9$) (unpaired *t*-test with Welch's correction).

established protocol and performed flow cytometry analysis.[32] We used DAPI to exclude the dead cells in the single-cell gate (*Figure 2A*). Then, we used CD45 to identify the immune cell populations, in which the $CD45^{high}$ population is blood-derived infiltrated leukocytes, and the $CD45^{medium}$ population is the endogenous microglia[32] (*Figure 2B–E*). Based on the cell size, $CD45^{high}$ leukocytes were divided into two populations, myeloid cells and lymphocytic cells. Myeloid cells were divided into neutrophils and monocytes based on the neutrophil marker Ly6G, and lymphocytic cells were divided into B cells, T cells, and NK cells based on the B cell marker CD19 and the T cell marker CD3e (*Figure 2B–E*). Ly6C was used to identify the activation status of monocytes and microglia (*Figure 2B–E*).

We found that eM2KO did not alter the immune cell populations in the contralateral hemisphere (control side) 24 h after MCAO but inhibited the increase of blood leukocyte infiltration into the ipsilateral hemisphere (infarction side) (*Figure 2D–F*). The composite roles of T cells in ischemic stroke remain controversial, but the overall effects of T cells in the early stages of ischemic stroke is proinflammatory and can aggregate tissue injury.[33] We found that compared to the WT mice, T cell infiltration after MCAO was inhibited by eM2KO (*Figure 2D*, *E*, and *H*). We barely detected any B cells in the brains (*Figure 2B–E*), indicating that our isolation is successful as there is no contamination of B cells from the blood or lymph nodes. NK cell infiltration also promotes ischemic brain injury.[34] We found that the increased infiltration of $CD3e^{-}CD19^{-}$ lymphocytic cells in WT mice after MCAO was reduced in eM2KO mice (*Figure 2D*, *E*, and *I*), suggesting that NK cell invasion was attenuated.

Neutrophils are the first immune cells to arrive during an ischemic stroke within hours and aggravate the brain injury.[35] We found that the enhanced infiltration of $CD11b^{+}Ly6G^{+}$ neutrophils after MCAO in WT mice was attenuated in eM2KO mice (*Figure 2D*, *E*, and *J*), which was confirmed by myeloperoxidase (MPO, a neutrophil marker) staining of the penumbra (see Supplementary material online, *Figure S2E and F*). Also, WB analysis showed that the increased expression of MPO in the brain after MCAO was attenuated by eM2KO (see Supplementary material online, *Figure S2I and J*). After ischemic stroke, monocyte/macrophage infiltration happens within 12 h and causes a long-term inflammatory response.[35] We found that infiltration of $CD11b^{+}Ly6G^{-}$ monocytes after MCAO was suppressed in eM2KO mice (*Figure 2D*, *E*, and *K*), which was also examined by F4/80 staining (see Supplementary material online, *Figure S2G and H*) and WB analysis of CD11b (see Supplementary material online, *Figure S2I and J*).

Not surprisingly, compared with WT mice, in eM2KO mice, we observed an inhibition of the mRNA expression of inflammatory chemokines *Ccl2* (*Mcp1*), *Cxcl1*, and *Cxcl2* (see Supplementary material online, *Figure S2K*), as well as the reduced protein expression of MCP1 (see Supplementary material online, *Figure S2L and M*). In summary, the above results suggest that *Trpm2* deletion in endothelial cells protects against ischemic brain injury by mitigating BBB leakage and inflammatory infiltration.

## 3.3 *Trpm2* deletion prevents CEC hyperpermeability induced by OGD

Besides endothelial dysfunction, many other factors, such as immune cell invasion and glutamate excitotoxicity, also contribute to the disruption of BBB during ischemic stroke.[7] Therefore, it is necessary to examine the role of TRPM2 in endothelial permeability by *in vitro* experiments using isolated primary cells. CECs were isolated based on a well-developed protocol.[36] We used OGD to treat CECs, as OGD can better mimic *in vivo* ischemic injury condition compared with $H_2O_2$ treatment.[37] We found that a 4- or 8-h OGD markedly down-regulated the mRNA expression of tight junction markers *Zo1*, *Claudin5*, and *Occludin* (see Supplementary material online, *Figure S3A*) and reduced the protein expression of occludin (*Figure 3A* and *B*) in WT CECs but not in TRPM2-KO CECs (see Supplementary material online, *Figure S3A*; *Figure 3A* and *B*). As the 8-h OGD treatment caused an unnecessary increase of CEC death, we chose to use 4 h as our treatment duration. Interestingly, different to the increased expression of proinflammatory chemokines *in vivo*, TRPM2 knockout did not inhibit the OGD-induced up-regulation of *Ccl2* and *Cxcl1* in CECs *in vitro* (see Supplementary material online, *Figure S3D*), suggesting that endothelial cells may not be the major source of chemokine production during ischemic stroke.

To evaluate endothelial permeability,[38] CECs were plated onto the upper chamber of transwell inserts with pore sizes of 0.4 μm. When endothelial cells completely covered the upper surface of inserts 3–5 days after seeding, either a 4-h OGD or control treatment was applied to the cells, and endothelial permeability was evaluated by adding Evans blue to the upper chamber (see Supplementary material online, *Figure S3C*). A marked leakage of Evans blue into the lower chamber was induced by OGD in CECs isolated from WT mice, but this leakage was inhibited in the CECs isolated from eM2KO (*Figure 3C*). These results suggest that deletion of *Trpm2* inhibits the increase in endothelial permeability after OGD, which is consistent with the *in vivo* results showing the reduced leakage in MCAO brain in *Trpm2* deletion mice (*Figure 1*).

We next used *in vitro* macrophage infiltration assay to further examine endothelial permeability to immune cells.[39] CECs were plated onto transwell inserts with pore sizes of 12 μM for macrophage migration. After endothelial cells were exposed to OGD or control treatment for 4 h, bone marrow–derived macrophages (BMDMs) were added into the upper chamber, while C5a was added into the lower chamber to promote macrophage infiltration. The infiltrated BMDMs on the 25 mm coverslips in the lower chamber were examined 12 h later by immunostaining with the macrophage marker F4/80 and the proinflammatory macrophage (M1) marker CD80 (see Supplementary material online, *Figure S3D*). We found that OGD treatment markedly increased the infiltration of macrophages into the lower chamber (*Figure 3D* and *E*), suggesting the degradation of tight junctions between CECs. Importantly, there were much fewer macrophages detected in the lower chamber in eM2KO group (*Figure 3D* and *E*), suggesting that *Trpm2* deletion cells prevent tight junction degradation caused by OGD. These results recapitulate our *in vivo* data that *Trpm2* deletion inhibits immune cell invasion after MCAO.

## 3.4 *Trpm2* deletion inhibits OGD-induced cellular stress in CECs

Next, we sought to understand how *Trpm2* deletion prevents endothelial dysfunction. Nitric oxide synthase 3 (NOS3), the endothelial cell–specific NOS (eNOS), produces nitric oxide (NO) during oxidative stress,[40] which can neutralize the over-produced reactive oxygen species (ROS), hence protecting CECs against ischemic injury.[40–42] Phosphorylation of NOS3 at Serine 1179 (pNOS3) increases NO production and minimizes ROS production,[40–42] whereas the ubiquitously expressed nitric oxide synthase 2 (NOS2), the inducible NOS (iNOS), promotes ROS production by causing NOS uncoupling during oxidative stress and increases CEC damage under ischemia.[40,43]

Although there was no significant increase of NOS3 phosphorylation, we found that the expression of NOS3 was increased in brains from WT mice 24 h after MCAO, suggesting the activation of endogenous protection mechanism against oxidative stress in CECs (*Figure 3F* and *G*). In contrast, compared to WT mice brains, the brains from eM2KO mice after MCAO showed a higher level of NOS3 expression and a marked increase of NOS3 phosphorylation (*Figure 3F* and *G*). We also examined NOS3 phosphorylation in the brain from mice with neuron-specific *Trpm2* deletion (nM2KO), which was found to protect mice from ischemic stroke in our previous work.[44] We found that, although there was a slightly higher increase of NOS3 expression in nM2KO after MCAO compared to WT mice, the observed increase of NOS3 phosphorylation in eM2KO mice was absent in nM2KO mice (see Supplementary material online, *Figure S3E and F*). This result suggests that the increased phosphorylation of NOS3 was not caused by mitigated tissue damage but was rather associated with the specific deletion of *Trpm2* in endothelial cells, and that TRPM2 activation in endothelial cells after MCAO inhibits NOS3 phosphorylation. Additionally, the pathologically heightened expression of NOS2 after MCAO was inhibited in eM2KO mice (*Figure 3F* and *G*).

NOS3 was also reported to be expressed in some neuronal cells.[45] To further confirm that the change in NOS3 expression and phosphorylation

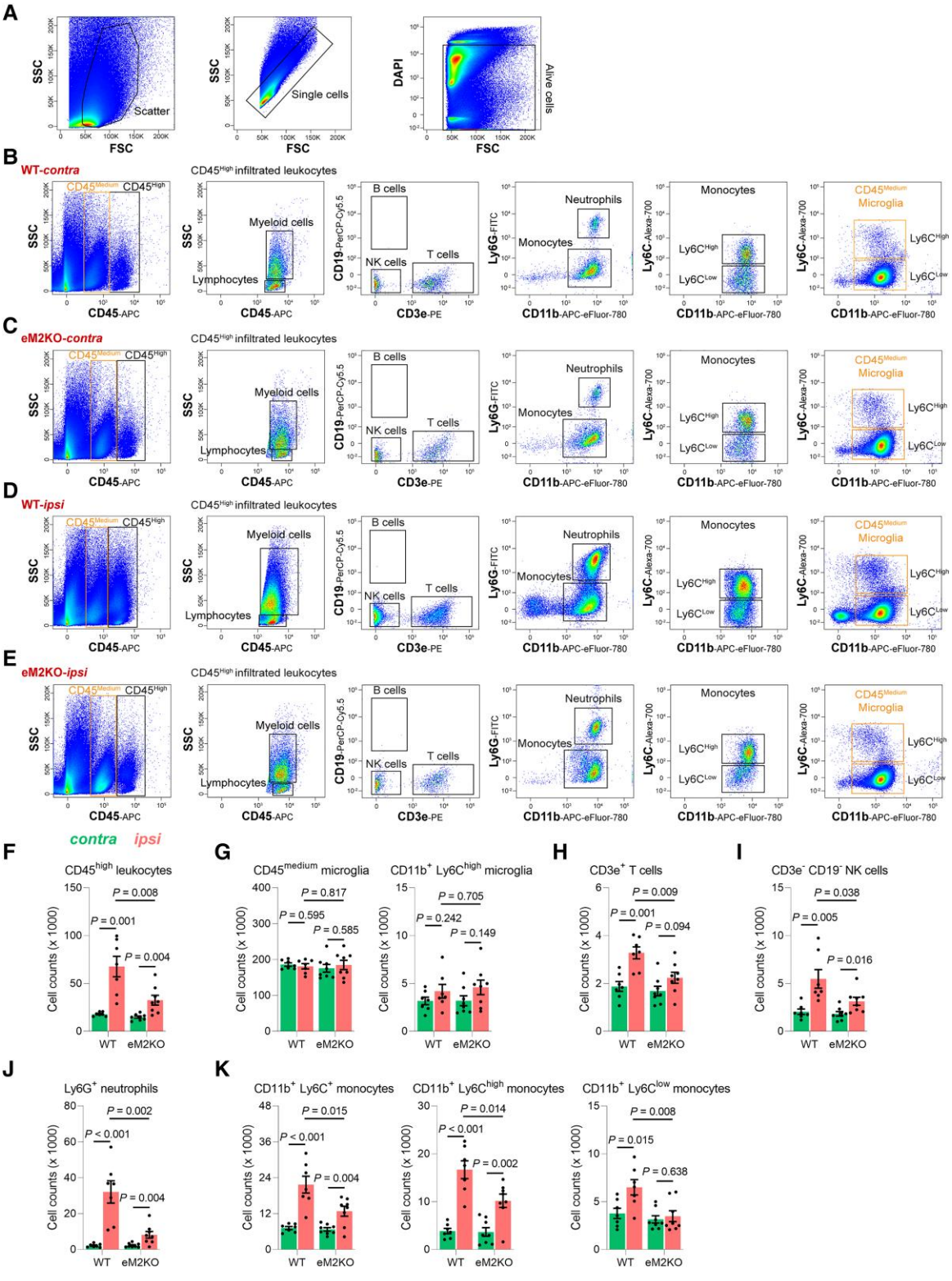


**Figure 2** *Trpm2* deletion attenuates post-stroke immune cell invasion. (*A*) Gating strategy of alive cells from single-cell suspension after brain digestion. Single cells were identified from the scatter gate, which were further divided into living cells and dead cells based on DAPI intensity. (*B–E*) Representative flow cytometry analysis of immune cell populations. Among alive cells, CD45 was used to identify nonimmune cells ($CD45^{-}$), microglia ($CD45^{medium}$), and leukocytes ($CD45^{high}$). Microglia were divided into two populations based on Ly6C expression. Leukocytes were divided into myeloid and lymphocytic cells based on cell size. Lymphocytes were divided into B cells, T cells, and NK cells based on CD19 and CD3e. Myeloid cells were divided into neutrophils and monocytes based on Ly6G. Monocytes were further divided into two populations based on Ly6C expression. Quantification of $CD45^{high}$ leukocytes (*F*), $CD45^{medium}$ microglia (*G*), $CD3e^{+}$ T cells (*H*), $CD3e^{-}CD19^{-}$ NK cells (*I*), $Ly6G^{+}$ neutrophils (*J*), and $CD11b^{+}Ly6G^{-}$ monocytes (*K*) ($n = 9, 8$) (unpaired *t*-test with Welch's correction).

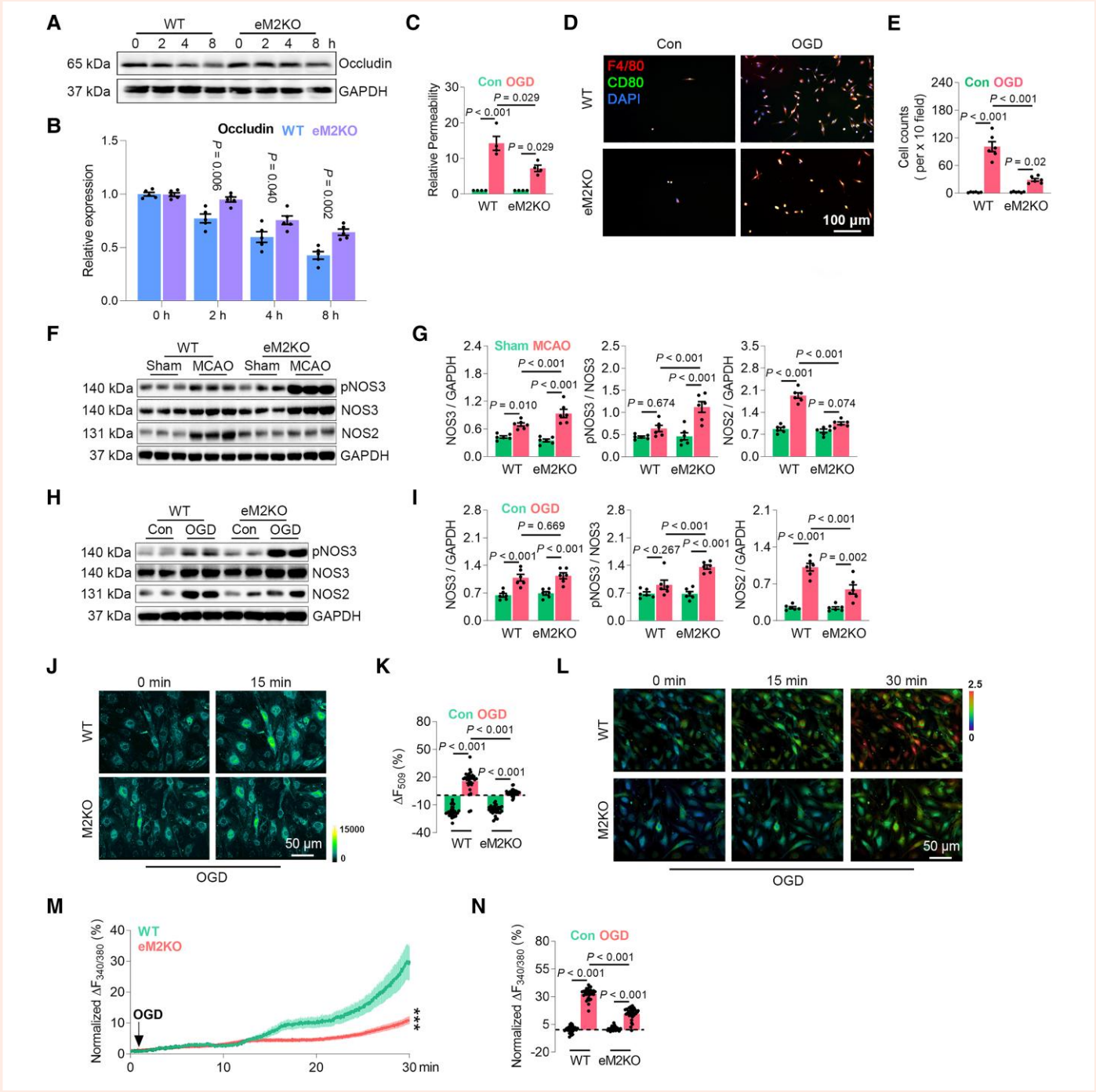


**Figure 3** *Trpm2* deletion prevents OGD-induced cerebral endothelial hyperpermeability. (*A*, *B*) *Trpm2* deletion preserved occludin expression. Representative WB analysis of the expression of occludin in CECs 2, 4, and 8 h after OGD ($n = 5$/group). (*C*) *In vitro* leakage assay as detailed in Supplementary material online, *Figure S3C*. Quantification of Evans blue absorption from lower chamber at 610 nm ($n = 6$/group). (*D*, *E*) *In vitro* macrophage infiltration assay as detailed in Supplementary material online, *Figure S3D*. F4/80 and CD80 staining of macrophages in lower chamber was performed as in (*D*). (*E*) Quantification of the number of infiltrated macrophages under ×10 field ($n = 6$/group). (*F*, *G*) WB analysis of the expression of pNOS3, NOS3, and NOS2 in the brain 24 h after sham surgery or MCAO ($n = 6$/group). (*H*, *I*) WB analysis of the expression of pNOS3, NOS3, and NOS2 in isolated CECs ($n = 6$/group). (*J*, *K*) *Trpm2* deletion inhibited ROS production in CECs. (*J*) Rh123 real-time imaging before and 15 min after OGD in CECs. (*K*) Quantification of changes of Rh123 fluorescence 15 min after OGD. WT ($n = 62$ for OGD, $n = 46$ for control) and M2KO ($n = 40$ for OGD, $n = 39$ for control) CECs were from four dishes of cultured cells isolated from three mice in each group. (*L*–*N*) *Trpm2* deletion inhibited $Ca^{2+}$ overload in CECs. (*L*) Representative images at 0, 15, and 30 min during OGD. (*M*) Averaged traces from 10 CECs. (*N*) Quantification of Fura-2 changes 30 min after OGD. WT ($n = 36$ for OGD, $n = 36$ for control) and M2KO ($n = 53$ for OGD, $n = 45$ for control) CECs were from four dishes of cultured cells isolated from three mice in each group (unpaired *t*-test with Welch's correction).

in the brain (*Figure 3F* and *G*) was attributed to endothelial cells, we examined NOS expression in isolated CECs subjected to OGD. We found that there was an increase in NOS3 phosphorylation in M2KO CECs compared with WT CECs (*Figure 3H* and *I*). Moreover, the increased expression of NOS2 induced by OGD was inhibited in M2KO CECs (*Figure 3H* and *I*). The increased NOS3 phosphorylation and reduced NOS2 expression in M2KO CECs predict an increased NO production but a decreased ROS production in response to OGD treatment.[40,43]

We next measured ROS production in CECs using Rhodamine-123 (Rh123), a commonly used dye for monitoring mitochondria membrane potential and ROS production.[46] Ischemia causes mitochondria membrane depolarization[47] and mitochondrial dysfunction,[48] which transform mitochondria into ROS production machines.[49,50] We found that OGD induced a marked increase of Rh123 fluorescence in WT CECs in 15 min, but this increase was inhibited in eM2KO CECs (*Figure 3J* and *K*), suggesting the preserved mitochondrial function and reduced ROS production in M2KO CECs.

One major cause of mitochondria depolarization and dysfunction is $Ca^{2+}$ overload.[7] Thus, we measured intracellular $Ca^{2+}$ concentration using real-time ratio $Ca^{2+}$ imaging. OGD induced a sustained increase of intracellular $Ca^{2+}$ in WT CECs, but this increase was suppressed in eM2KO CECs (*Figure 3L–N*). In summary, we found that M2KO preserved mitochondria function, inhibited ROS production, and mitigated $Ca^{2+}$ overload in CECs subjected to OGD.

## 3.5 *Trpm2* deletion inhibits CD36 activation by OGD and TSP1 in CECs

We subsequently investigated the underlying molecular mechanisms of M2KO-mediated protection against endothelial dysfunction and hyperpermeability. We found that OGD markedly increased the expression of TRPM2 by 4.24-fold (see Supplementary material online, *Figure S4A and B*), which is consistent with our previous report that the expression of TPRM2 in the brain is substantially up-regulated after MCAO.[44] Another member of the TRPM family, TRPM4, was also found to promote endothelial dysfunction during ischemic stroke.[51] We found that the basal expression level of TRPM4 appeared to be much higher than TRPM2 (see Supplementary material online, *Figure S3H and I*). Similar to TRPM2, the expression of TRPM4 was also up-regulated by OGD, but this increase (1.48-fold) is smaller than TRPM2 (see Supplementary material online, *Figure S4A and B*). After a 4-h OGD treatment, we also recorded much greater TRPM2 current in CECs (see Supplementary material online, *Figure S3C and D*). Our results suggest that although TRPM4 has a higher expression level than TRPM2 in CECs under physiological conditions, TRPM2 expression can be substantially enhanced to a further extent by a pathological stimulus.

Endothelial hyperpermeability after ischemic stroke can be induced by various signaling pathways including CD36.[52] We found that CD36 expression in the brain was increased by MCAO, but this increase was inhibited by *Trpm2* deletion (see Supplementary material online, *Figure S4E and F*). Considering immune cells have a high expression of CD36, we performed OGD using isolated CECs to better examine the role of CD36 in endothelial dysfunction. Our results show that CD36 expression was increased in WT CECs by OGD but not in eM2KO CECs (*Figure 4A* and *B*). Importantly, the basal expression level of CD36 in the brain and CECs is not significantly altered by eM2KO (*Figure 4A* and *B*; Supplementary material online, *Figure S4E and F*).

Activation of CD36 triggers downstream signaling of factors associated with oxidative stress, ROS production, and cell death, including Fyn, JNK, and p38.[17,53,54] We found that in WT CECs exposed to OGD, phosphorylation of Fyn, JNK, and p38 was markedly increased, whereas this increase was inhibited in eM2KO CECs (*Figure 4A* and *B*), suggesting that TRPM2 is critical for CD36 signaling activation induced by OGD. Since OGD can also cause many nonspecific cellular responses, we further examined the role of TRPM2 in CD36 activation in CECs using a CD36 ligand thrombospondin-1 (TSP1). TSP1 is a glycoprotein that can be secreted by endothelial cells, and the production of TSP1 in endothelial cells increases rapidly within hours following tissue injury or inflammation, leading to endothelial cell apoptosis during ischemic stroke.[55–57] Moreover, TSP1–CD36 signaling was found to increase endothelial hyperpermeability induced by vascular endothelial growth factor (VEGF).[58] We observed that a 4-h TSP1 treatment at 1 μg/mL induced a robust activation of CD36 signaling cascades in WT CECs, which was inhibited in M2KO CECs (*Figure 4C* and *D*).

Similar to OGD-induced responses, TSP1 increased NOS3 expression in both WT and eM2KO CECs but only promoted NOS3 phosphorylation in M2KO CECs (*Figure 4E* and *F*). This increased NOS2 expression induced by TSP1 was inhibited by M2KO (*Figure 4E* and *F*). TSP1 also induced a rapid increase of Rh123 fluorescence in WT endothelial cells, whereas this increase was blunted in M2KO CECs (*Figure 4G* and *H*), suggesting that TRPM2 promotes TSP1-mediated ROS production in mitochondria. Moreover, TSP1 perfusion induced a sustained increase of intracellular $Ca^{2+}$ in WT CECs, which was inhibited by *Trpm2* deletion (*Figure 4I–K*). These results indicate that TRPM2 is critical in magnifying TSP1-induced oxidative stress in CECs.

TSP1 treatment for 4 h caused a significant loss of occludin in WT CECs but not in M2KO CECs (*Figure 4L* and *M*). In *in vitro* permeability assay (see Supplementary material online, *Figure S3E and F*), TSP1 resulted in a moderate increase of Evans blue leakage (*Figure 4N*) compared to that caused by OGD (*Figure 3C*), and this increase was inhibited in M2KO CECs (*Figure 4N*). Similar to OGD-induced macrophage infiltration (*Figure 3D* and *E*), TSP1 also induced macrophage infiltration in WT CECs, which was inhibited in M2KO CECs (*Figure 4O*).

Ultimately, our data indicate that CD36 activation promotes endothelial hyperpermeability, and that TRPM2 is critical for the activation of CD36 signaling cascade during OGD.

## 3.6 Inhibiting TRPM2 suppresses CD36 activation in CECs

The observation of TRPM2-dependent CD36 activation makes us ask whether TRPM2 is activated during OGD and TSP1 treatment. We recorded TRPM2 current during OGD or TSP1 perfusion. The pipette solutions for TRPM2 recording contained 500 nM $Ca^{2+}$ and 1 μM ADPR, which could not elicit TRPM2 current in HEK293 cells over-expressing TRPM2 without OGD treatment (*Figure 5A* and *B*). We used *N*-(*p*-amylcinnamoyl)anthranilic acid (ACA) to confirm TRPM2 current and NMDG to determine any involvement of leak current. We found that OGD treatment induced TRPM2 activation in HEK293T cells co-expressed with CD36 but not in HEK293T cells expressed with TRPM2 alone (*Figure 5A–C*). The OGD-induced activation of TRPM2 currents was inhibited by preincubation with a CD36-specific inhibitor, sulfosuccinimidyl oleate (sodium salt) (SSO) (*Figure 5C*; Supplementary material online, *Figure S4G*).

To understand how CD36 promotes TRPM2 activation by OGD, we investigated whether OGD and CD36 influence intracellular $Ca^{2+}$ or ADPR, two critical factors required for the activation of TRPM2.[59] We used the PLC inhibitor U73122 to inhibit intracellular $Ca^{2+}$ release and used a potent poly ADPR-ribose polymerase inhibitor, PJ34, to prevent ADPR production during OGD treatment. We found that preincubation of PJ34 and U73122 (in the presence of $Ca^{2+}$ free extracellular recording solution) largely eliminated TRPM2 activation induced by OGD (*Figure 5C*; Supplementary material online, *Figure S4G*). As *Trpm2* deletion markedly inhibited CD36 activation (*Figure 4*), we investigated whether inhibition of TRPM2 by ACA, PJ34, and U73122 also produces a similar effect. CECs incubated with ACA, PJ34, and U73122 displayed reduced activation of CD36 signaling after OGD treatment (*Figure 5D* and *E*).

TSP1 also activates TRPM2 current in HEK293T cells co-transfected with TRPM2 and CD36 (*Figure 5F* and *H*) but not in HEK293T cells transfected with TRPM2 alone (*Figure 5G*). Preincubation with SSO abolished the activation of TRPM2 by TSP1 (*Figure 5H*; Supplementary material online, *Figure S4H*). Similar to OGD, the activation of TRPM2 by TSP1 was eliminated when transfected cells were preincubated with ACA, PJ34, and U73122 (*Figure 5H*; Supplementary material online, *Figure S4H*). The activation of CD36 signaling cascades in CECs by TSP1 was blocked by inhibiting TRPM2 with ACA, PJ34, and U73122 (*Figure 5H*; Supplementary material online, *Figure S4H*).

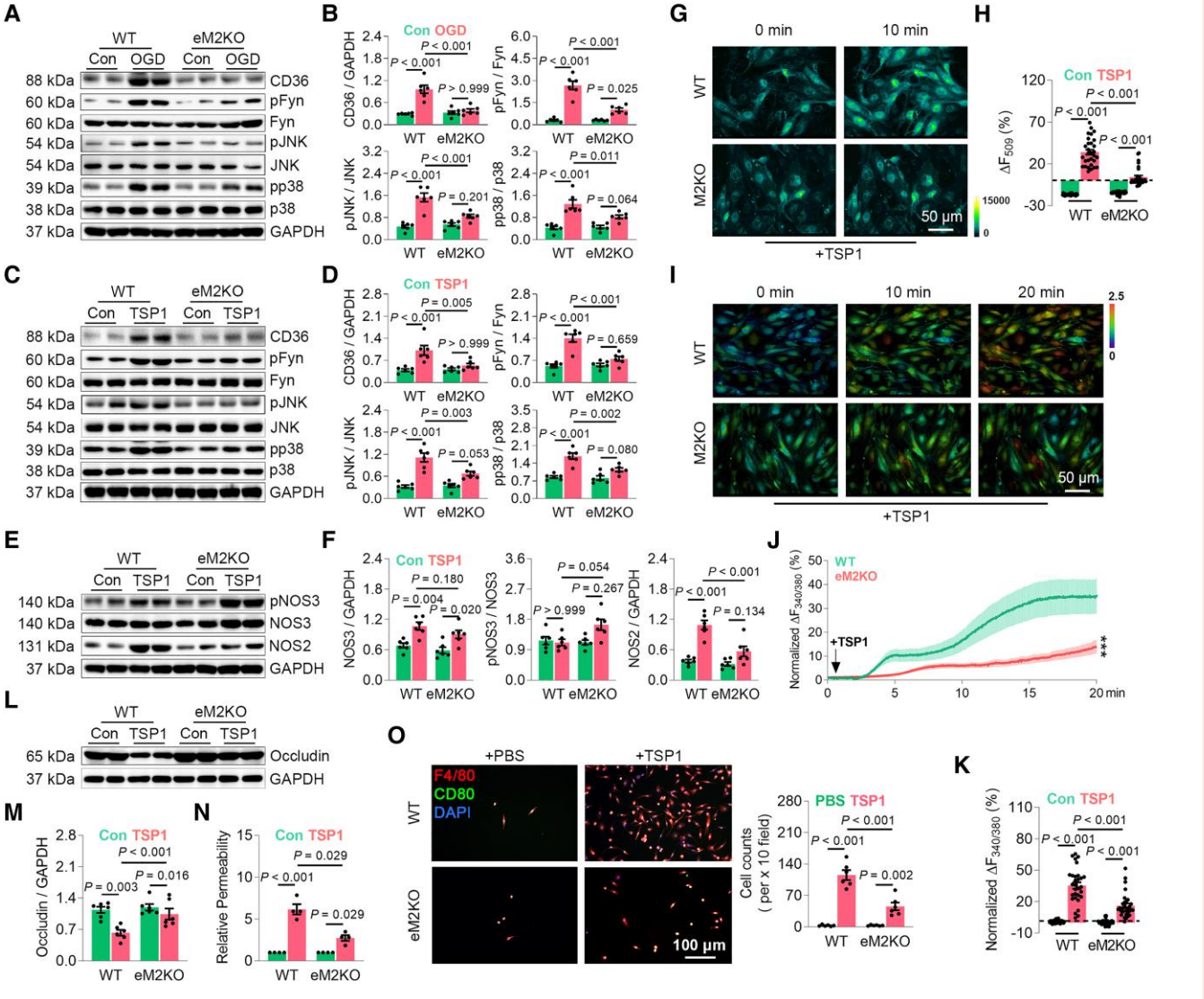


**Figure 4** *Trpm2* deletion suppresses CD36 signaling activation. WB analysis of the expression of CD36, pFyn, Fyn, pJNK, JNK, pp38, and p38 in CECs subjected to OGD (*A*, *B*) and TSP1 (*C*, *D*) treatment ($n = 6$/group). (*E*, *F*) WB analysis of the expression of pNOS3, NOS3, and NOS2 in CECs ($n = 6$/group). (*G*) Rh123 imaging before and 10 min after TSP1 perfusion in CECs. (*H*) Quantification of Rh123 changes. WT ($n = 32$ for OGD, $n = 44$ for control) and M2KO ($n = 43$ for OGD, $n = 33$ for control) CECs were from four dishes isolated from three mice in each group. (*I*) Representative images at 0, 10, and 20 min during TSP1 perfusion. (*J*) Averaged traces were from 10 CECs. (*K*) Quantification of Fura-2 changes 20 min after TSP1 perfusion. WT ($n = 31$ for OGD, $n = 62$ for control) and M2KO ($n = 32$ for OGD, $n = 40$ for control) CECs were from four dishes isolated from three mice in each group. (*L*, *M*) WB analysis of the expression of occludin in CECs ($n = 6$/group). (*N*) Quantification of *in vitro* endothelial cell permeability test (as in Supplementary material online, *Figure S3E*). (*O*) *In vitro* macrophage infiltration test (as in Supplementary material online, *Figure S3F*) (unpaired *t*-test with Welch's correction).

The above data suggest that during OGD and TSP1 treatment, CD36 promotes TRPM2 activation by increasing ADPR production and intracellular $Ca^{2+}$ concentration. Moreover, TRPM2-mediated $Ca^{2+}$ signaling is also required for the activation of CD36 signaling cascades, which is similar to the critical role of TRPM2-mediated $Ca^{2+}$ in many other cellular functions.[60]

## 3.7 Inhibition of TRPM2 or CD36 prevents endothelial dysfunction induced by OGD and TSP1

Continuously, we examined whether inhibiting TRPM2 activation influences the phenotypic changes of CECs induced by OGD or TSP1 treatment. Preincubating CECs with SSO promoted NOS3 phosphorylation and inhibited the increase of NOS2 induced by either OGD (see Supplementary material online, *Figure S5A* and *B*) or TSP1 treatment (see Supplementary material online, *Figure S5C* and *D*). Using TRPM2 inhibitor ACA or inhibiting the activation of TRPM2 using PJ34 or U73122 produced similar effects on the expression of pNOS3 and NOS2 in CECs subjected to OGD (see Supplementary material online, *Figure S5A* and *B*) and TSP1 perfusion (see Supplementary material online, *Figure S5C* and *D*). SSO, ACA, PJ34, and U73122 also mitigated the mitochondrial depolarization and ROS production in CECs induced by either OGD (*Figure 6A* and *C*) or TSP1 treatment (*Figure 6B* and *D*). Moreover, the increase of intracellular $Ca^{2+}$ in CECs induced by either OGD (*Figure 6E* and *G*) or TSP1 treatment (*Figure 6F* and *H*) was inhibited by SSO, ACA, PJ34, and

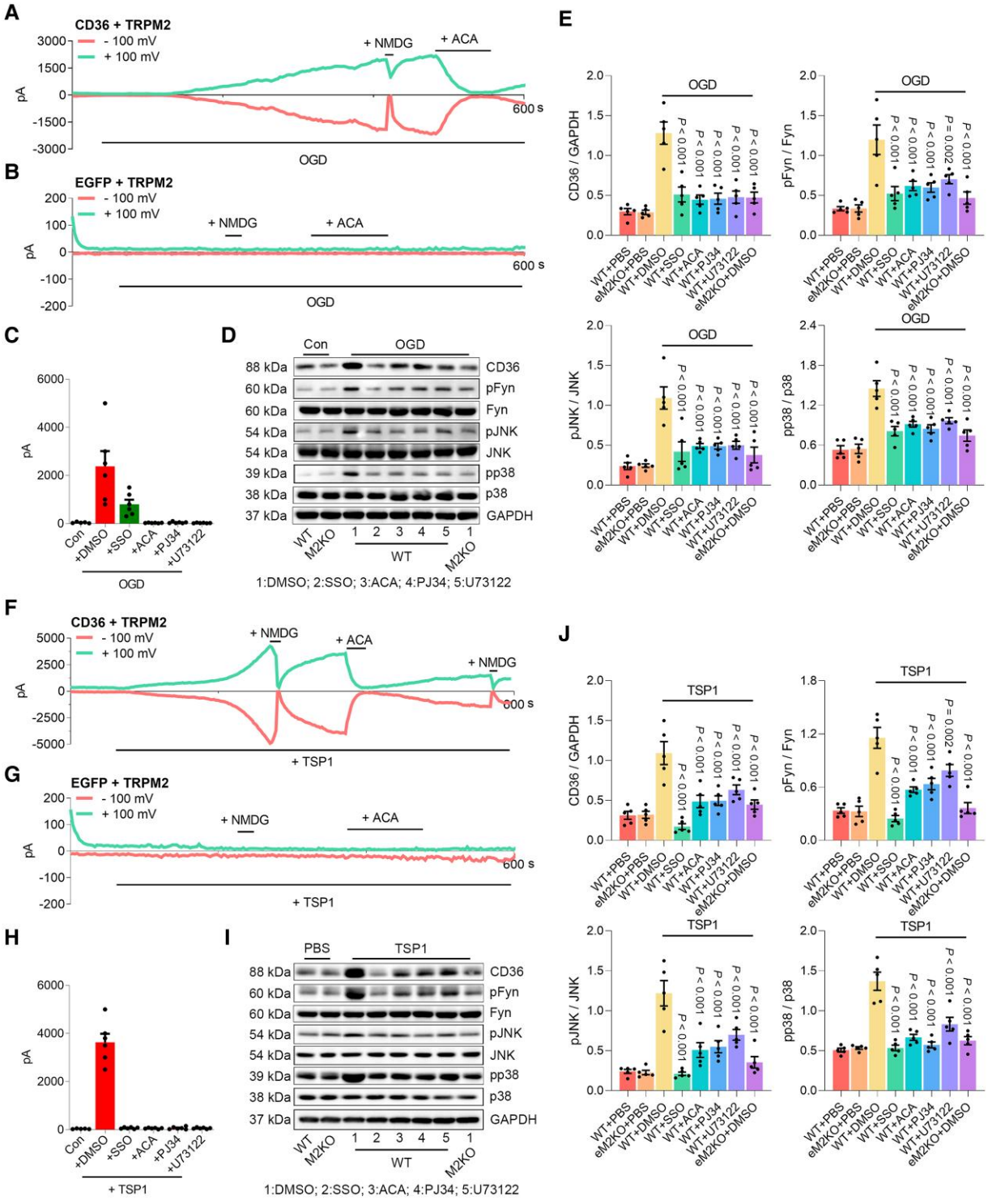


**Figure 5** Inhibiting the activation of TRPM2 suppresses the activation of CD36 signaling cascades in CECs. (*A*) Representative TRPM2 current traces elicited by OGD (upper trace: outward current at +100 mV; lower trace: inward current at +100 mV) in HEK293T cells transfected with CD36 and TRPM2. NMDG blocks inward current indicating the tightness of seal. ACA is a TRPM2 channel blocker. (*B*) Representative recording traces in HEK293T cells transfected with only TRPM2 during OGD. (*C*, *H*) Quantification of TRPM2 current amplitude in HEK293T cells transfected with CD36 and TRPM2 during OGD as in (*C*) and during TSP1 treatment as in (*H*) ($n = 6$/group). (*D*, *E*) Representative WB analysis of the expression of CD36, pFyn, Fyn, pJNK, JNK, pp38, and p38 in CECs ($n = 5$/group). (*F*) Representative TRPM2 current traces (upper trace: outward current at +100 mV; lower trace: inward current at +100 mV) in HEK293T cells transfected with CD36 and TRPM2 during TSP1 treatment. NMDG blocks inward current indicating the tightness of seal. ACA is a TRPM2 blocker. (*G*) Representative recording traces in HEK293T cells transfected with only TRPM2 during TSP1 treatment. (*I*, *J*) (*I*) Representative WB of the expression of CD36, pFyn, Fyn, pJNK, JNK, pp38, and p38 in CECs ($n = 5$/group) (two-way Welch ANOVA with Dunnett's T3 test).

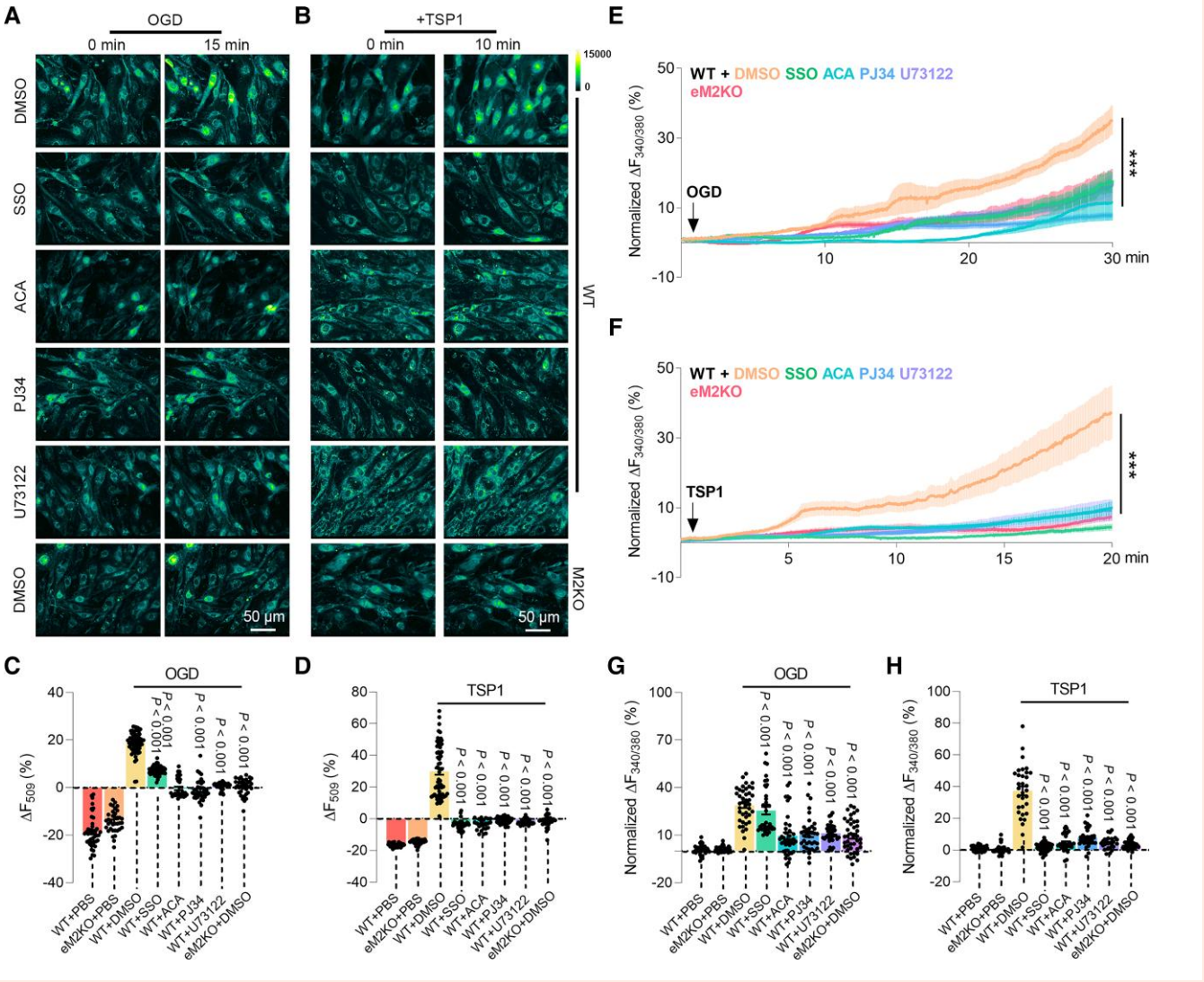


**Figure 6** TRPM2 inhibition prevents oxidative stress and $Ca^{2+}$ overload in endothelial cells after OGD or TSP1 treatment. (*A–D*) Representative picture of Rh123 imaging before and 15 min after OGD as in (*A*) and 10 min after TSP1 treatment as in (*B*) in isolated CECs with the treatment of DMSO, SSO, ACA, PJ34, and U73122. Quantification of changes of Rh123 fluorescence 15 min after OGD as in (*C*) and 5 min after TSP1 treatment as in (*D*) ($n = 30–50$/group). (*E–H*) Representative real-time Fura-2 $Ca^{2+}$ imaging traces during OGD as in (*E*) and during TSP1 treatment as in (*F*) with the treatment of DMSO, SSO, ACA, PJ34, and U73122. The averaged traces were from 10 CECs. Quantification of Fura-2 fluorescence changes 30 min after OGD as in (*G*) and 20 min after TSP1 treatment as in (*H*) ($n = 30–50$/group) (two-way Welch ANOVA with Dunnett's T3 test).

U73122 preincubation. These results suggest that inhibiting TRPM2 produced a similar protective effect against oxidative stress in CECs induced by OGD as *Trpm2* deletion.

As NOS activity does not directly reflect NO generation, we directly measured NO production using DAF-FM in CECs subjected to OGD.[61] The results showed that TRPM2 knockout or inhibition of TRPM2 activation preserved the compromised NO production in CECs induced by OGD (see Supplementary material online, *Figure S6A and B*) or TSP1 (see Supplementary material online, *Figure S6C and D*). Moreover, we used MitoSOX to directly evaluate mitochondrial ROS generation in CECs during OGD[62] and found that the MitoSOX increase induced by OGD (see Supplementary material online, *Figure S6E and F*) or TSP1 (see Supplementary material online, *Figure S6G and H*) was suppressed by TRPM2 knockout or inhibition of TRPM2 activation.

Next, we tested whether the inhibition of TRPM2 preserves endothelial permeability. We found that SSO, ACA, PJ34, and U73122 inhibited the loss of occludin in WT CECs subjected to OGD (see Supplementary material online, *Figure S7A and B*) and TSP1 treatment (see Supplementary material online, *Figure S7C and D*). In *in vitro* endothelial permeability test, SSO, ACA, PJ34, and U73122 markedly decreased Evans blue leakage (see Supplementary material online, *Figure S7E and F*). Macrophage infiltration across CECs undergoing OGD (see Supplementary material online, *Figure S7G and H*) and TSP1 treatment (see Supplementary material online, *Figure S7I and J*) was also antagonized by SSO, ACA, PJ34, and U73122.

## 3.8 TRPM2 inhibition prevents post-stroke BBB leakage

ACA is a nonspecific TRPM2 inhibitor and can inhibit the activation of other channels, and SSO, PJ34, and U73122 did not directly inhibit TRPM2 activation. To further confirm the translational value of TRPM2 inhibition against endothelial dysfunction, we used a highly selective TRPM2 inhibitory peptide, TAT-M2. TAT-M2 works by blocking the binding of

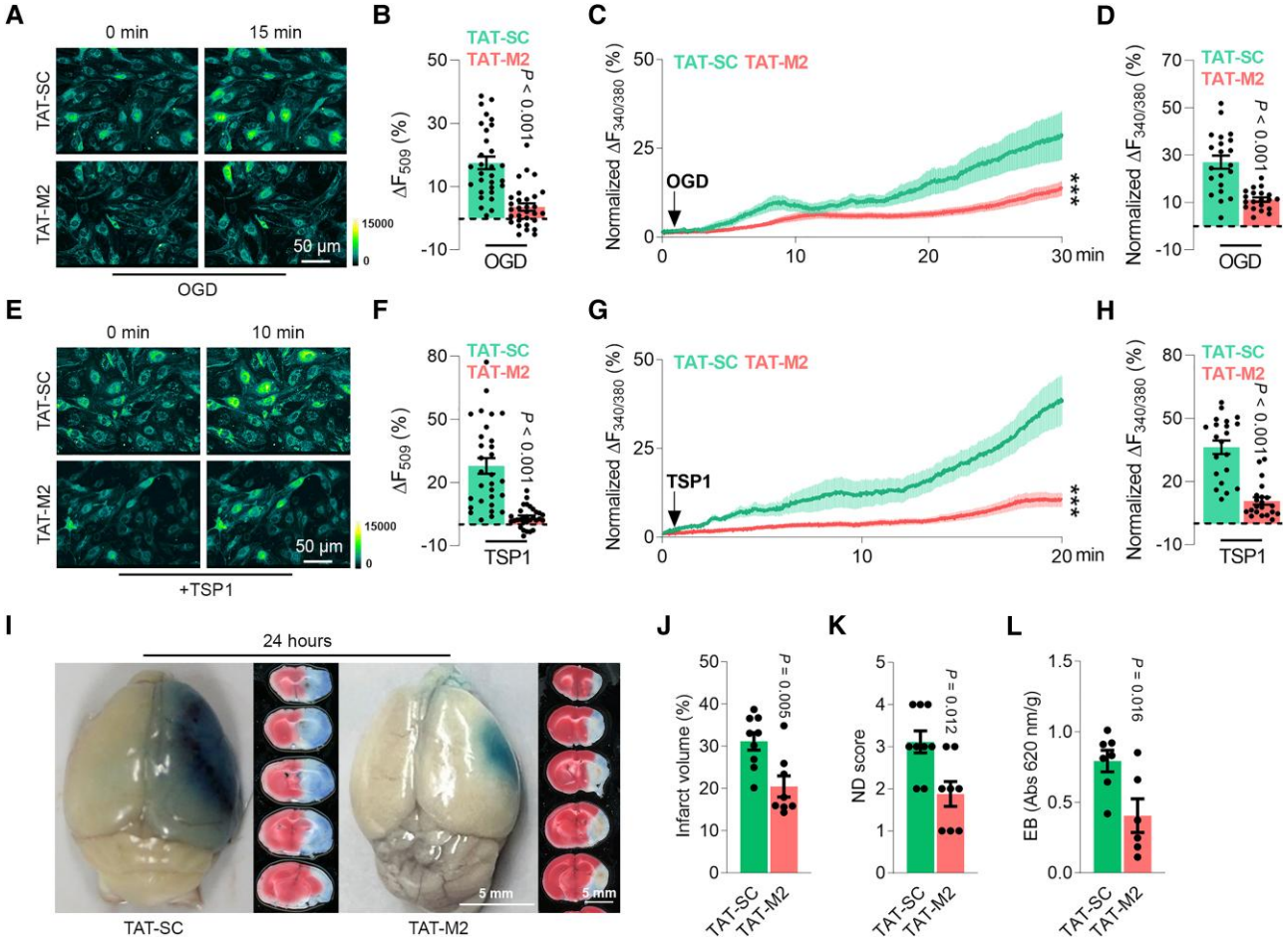


**Figure 7** TRPM2 inhibition preserves BBB integrity *in vivo*. (*A–D*) Rh123 imaging and Fura-2 $Ca^{2+}$ imaging after OGD. (*A*) Representative Rh123 images before and 15 min after OGD. (*B*) Quantification of changes of Rh123 fluorescence 15 min after OGD ($n = 20–30$/group). (*C*) Representative real-time Fura-2 $Ca^{2+}$ imaging traces during OGD from 10 CECs. (*D*) Quantification of Fura-2 fluorescence changes 30 min after OGD ($n = 20–30$/group). (*E–H*) Rh123 imaging and Fura-2 $Ca^{2+}$ imaging after TSP1 treatment. (*E*) Representative Rh123 images before and 10 min after TSP1 treatment. (*F*) Quantification of changes of Rh123 fluorescence 15 min after TSP1 treatment ($n = 20–30$/group). (*G*) Representative real-time Fura-2 $Ca^{2+}$ imaging traces during TSP1 treatment from 10 CECs. (*H*) Quantification of Fura-2 fluorescence changes 20 min after TSP1 treatment ($n = 20–30$/group). (*I*) Evans blue assay and TTC staining of brain slices (1 mm). (*J*, *K*) Mean infarct volume and average ND score after MCAO from TAT-SC ($n = 9$) and TAT-M2 mice ($n = 8$). (*L*) Quantification of Evans blue assay after MCAO from WT ($n = 7$) and eM2KO mice ($n = 6$) (unpaired *t*-test with Welch's correction).

ADPR to TRPM2, and it has been shown to attenuate ischemic stroke in mice.[63,64] We found that compared to the scramble control (TAT-SC), TAT-M2 effectively inhibited the mitochondrial ROS production and $Ca^{2+}$ overload induced by OGD (*Figure 7A–D*) or TSP1 treatment (*Figure 7E–H*) in CECs. Although TAT-M2 was shown to reduce the brain infarction after ischemic stroke in mice, but whether TAT-M2 produced other beneficial effects was undetermined.[63,64] We found that besides attenuating brain injury, TAT-M2 prevented the compromise of neurological functions 24 h after MCAO (*Figure 7I–K*). Also, TAT-M2 effectively inhibited Evans blue leakage (*Figure 7I* and *L*), suggesting that BBB integrity was preserved by TAT-M2.

In conclusion, our results suggest that the inhibition of TRPM2 is a promising therapeutic strategy in mitigating BBB degradation during ischemic stroke.

# 4. Discussion

The primary goal of therapies for ischemic stroke is to protect affected neurons. However, the failure of current treatments to directly inhibit neuronal death for mitigating ischemic brain injury is shifting researchers' attention to non-neuronal cells.[6] The NVU is a relatively new concept that emphasizes the importance of maintaining the homeostasis of the local microenvironment in the brain.[8,14] Endothelial cells compose the core component of the NVU and BBB, and endothelial hyperpermeability is a hallmark of brain damage during the early stages of ischemic stroke. This endothelial hyperpermeability drives the initial pathological changes of ischemic stroke as well as contributes to neuronal death.[65] However, the molecular mechanisms underlying endothelial dysfunction remain obscure.[14]

Global TRPM2 knockout protects mice against ischemic stroke, but the underlying mechanisms are still unclear.[66] Wild-type mice transplanted with bone marrow from *Trpm2* knockout mice exhibited reduced brain injury after MCAO,[25] implying an important role of TRPM2 in core processes of ischemic stroke, including immune cell invasion and activation. Similarly, our previously published work showed that specific knockout of TRPM2 in myeloid lineage cells using *CD11b-cre* attenuates atherosclerosis in mice by inhibiting macrophage infiltration and activation.[39] Moreover, we recently found that neuronal TRPM2 aggravates brain injury by enhancing glutamate excitotoxicity.[44] Recently, methamphetamine and

HIV-Tat protein were found to synergistically induce oxidative stress in CECs.[67] In this study, we demonstrated that selective deletion of *Trpm2* in endothelial cells also effectively protects mice against ischemic stroke. This is the first study to report that TRPM2 in CECs plays a key role in ischemic stroke. Our results suggest that targeting TRPM2 could produce a comprehensive protective effect against ischemic stroke.

The role of TRPM2 in causing endothelial hyperpermeability has only been shown in lung-derived endothelial cells *in vitro* in response to $H_2O_2$ stimulation.[24] However, $H_2O_2$ treatment at a high concentration (300 μM) is not an ideal simulation of oxidative stress during *in vivo* ischemia.[24] In our study, we utilized OGD, which better mimics ischemic conditions.[37] We also used CECs instead of pulmonary endothelial cells, the latter of which are prone to hyperpermeability due to their loose tight junction, abundant fenestrations, and frequent pinocytotic activity.[7]

Phosphorylation of NOS3 at S1177 greatly enhances the activity of NOS3, and transgenic mice expressing the NOS3 S1177D, a phosphomimetic mutant, have been recently found to have robust NO production in the brain, which might protect the brain against oxidative stress.[68] We found that *Trpm2* deletion or TRPM2 inhibition resulted in a marked increase in the phosphorylation of NOS3 at S1177 in the brain after MCAO, or in cultured CECs exposed to OGD, which is consistent with the inhibited ROS production evaluated by Rh123 mitochondrial imaging. These results provide strong evidence that the inhibition or deletion of *Trpm2* protects against oxidative stress in CECs during ischemic stroke.

CD36 was shown to be critical for the $Ca^{2+}$ influx induced by $H_2O_2$ in lung microvascular endothelial cells.[69] Endothelial CD36 promoted neutrophil activation after ischemic stroke and exacerbated brain damage.[70] We found that in isolated CECs, CD36 signaling cascades in CECs were activated by OGD to a similar degree compared to those activated by CD36 ligand TSP1. Recent single-cell RNA sequencing work identifies a distinct but abundant endothelial cell population with high CD36 expression.[16] Our work suggests that $CD36^{high}$ endothelial population may be prone to ischemic damage during stroke. Future fluorescence-activated cell sorting (FACS) work using CD36 should lead to better understanding of the role of $CD36^{low}$ and $CD36^{high}$ endothelial cells in different physiological and pathological conditions.

Previously, another CD36 ligand Aβ has been shown to induce TRPM2 activation in CECs, which caused neurovascular dysfunction in a Alzheimer's disease mouse model,[26] albeit the underlying mechanism of Aβ-induced TRPM2 activation is not clear. The most intriguing discovery in our study is the activation of TRPM2 by CD36. In conjunction, activation of CD36 by OGD and TSP1 also requires TRPM2-mediated $Ca^{2+}$ influx, suggesting the presence of a vicious TRPM2–CD36 cycle that enhances endothelial damage during ischemic stroke. This novel mechanism could also explain the Aβ-induced vascular damage in the development of Alzheimer's disease.

TSP1 is a secreted glycoprotein produced by many cell types including endothelial cells. TSP1 is known for its inhibition of VEGF signaling by activating CD36 in endothelial cells,[71] which causes inflammatory responses and induces apoptosis.[57] However, the underlying mechanisms regulating TSP1–CD36 signaling remain unclear. We found that *Trpm2* deletion inhibited TSP1-induced CEC dysfunction and hyperpermeability. Also, TSP1 activates TRPM2 in a CD36-dependent manner. These results indicate that the detrimental effects of TSP1 on CECs are dependent on TRPM2 activation.

Another member of the TRPM family, TRPM4, is also crucial in facilitating ischemic brain injury. Recently, TRPM4 was shown to be associated with the NMDA receptor by enhancing its excitotoxicity in neurons.[46] Moreover, in CECs, TRPM4 associates with sulfonylurea receptor 1 (Sur1), which promotes BBB degradation and increases brain injury during ischemic stroke.[72–74] The activation of TRPM4 requires a marked increase of intracellular $Ca^{2+}$,[75] and TRPM2 is highly permeable to $Ca^{2+}$. We found that TRPM2 knockout could produce a similar protective effect against ischemic stroke as TRPM4 inhibition, which suggests that TRPM2-mediated $Ca^{2+}$ signaling might be important for the activation of TRPM4.

One of the limitations of our study is using the young adult mice for MCAO model. As ischemic stroke is prevalent in elderly populations, our future studies will use aged mice and with comorbidities to better evaluate the therapeutic potential of targeting TRPM2 for ischemic stroke treatment.

In conclusion, we reveal that endothelial cell–specific TRPM2 knockout protects mice against ischemic stroke as evidenced by the reduced infarct volume and decreased plasma extravasation in the brain of mice subjected to MCAO. We discovered the mechanism by which deletion of *Trpm2* in endothelial cells protects mice against ischemic stroke is through inhibiting oxidative stress, preserving tight junctions between CECs, and reducing immune cell invasion in the brain. At the cellular level, *Trpm2* deletion protects CECs against oxidative stress and $Ca^{2+}$ overload and thereby preventing endothelial hyperpermeability induced by OGD or TSP1. At the molecular level, we identified a novel mechanism that TRPM2 and CD36 are inter-dependently activated when CECs are exposed to OGD or TSP1. Our results establish that targeting endothelial TRPM2 is a promising strategy in mitigating ischemic brain injury.

# Supplementary material

Supplementary material is available at *Cardiovascular Research* online.

# Authors' contributions

L.Y. and P.Z. conceived and designed the research. P.Z. performed most *in vitro* experiments. C.X.L did some *in vitro* experiments. E.R.J. helped in and gave advice on flow cytometry analysis. Z.Y. and J.F. performed the *in vivo* experiments. B.M. generated TRPM2 floxp mice and provided inputs to discussion. P.Z. and L.Y. wrote the manuscript. All authors commented on the manuscript.

## Acknowledgements

We thank Dr Andrew M. Scharenberg (University of Washington) for kindly providing TRPM2 plasmid. CD36-bio-His was a gift from Gavin Wright (Addgene plasmid #52025; http://n2t.net/addgene:52025; RRID: Addgene_52025).[76] The *Cdh5-CreERT2* mice[77] were kindly provided by Dr Ralf H. Adam (University of Munster). We thank Dr Rajkumar Verma for his advice on tomato staining.

**Conflict of interest:** None declared.

## Funding

This work was partially supported by the National Institute of Health (R01HL147350 and R01NS131661) and American Heart Association (19TPA34890022) to L.Y.

## Data availability

All data reported in this paper will be shared by the corresponding author upon request.

## References

1. Johnson CO, Nguyen M, Roth GA, Nichols E, Alam T, Abate D, Abd-Allah F, Abdelalim A, Abraha HN, Abu-Rmeileh NME, Adebayo OM, Adeoye AM, Agarwal G, Agrawal S, Aichour AN, Aichour I, Aichour MTE, Alahdab F, Ali R, Alvis-Guzman N, Anber NH, Anjomshoa M, Arabloo J, Arauz A, Ärnlöv J, Arora A, Awasthi A, Banach M, Barboza MA, Barker-Collo SL, Bärnighausen TW, Basu S, Belachew AB, Belayneh YM, Bennett DA, Bensenor IM, Bhattacharyya K, Biadgo B, Bijani A, Bikbov B, Bin Sayeed MS, Butt ZA, Cahuana-Hurtado L, Carrero JJ, Carvalho F, Castañeda-Orjuela CA, Castro F, Catalá-López F, Chaiah Y, Chiang PP-C, Choi J-YJ, Christensen H, Chu D-T, Cortinovis M, Damasceno AAM, Dandona L, Dandona R, Daryani A, Davletov K, de Courten B, De la Cruz-Góngora V, Degefa MG, Dharmaratne SD, Diaz D, Dubey M, Duken EE, Edessa D, Endres M, Faraon EJA, Farzadfar F, Fernandes E, Fischer F, Flor LS, Ganji M, Gebre AK, Gebremichael TG, Geta B, Gezae KE, Gill PS, Gnedovskaya EV, Gómez-Dantés H, Goulart AC, Grosso G, Guo T, Gupta R, Haj-Mirzaian A, Haj-Mirzaian A, Hamidi S, Hankey GJ, Hassen HJ, Hay SI, Hegazy MI, Heidari B, Herial NA, Hosseini MA, Hostiuc S, Irvani SSN, Islam SMS, Jahanmehr N, Javanbakht M, Jha RP, Jonas JB, Jozwiak JJ, Jürisson M, Kahsay A, Kalani R, Kalkonde Y, Kamil TA, Kanchan T, Karch A, Karimi N, Karimi-Sari H, Kasaeian A, Kassa TD, Kazemeini H, Kefale AT, Khader YS, Khalil IA, Khan EA, Khang Y-H, Khubchandani J, Kim D, Kim YJ, Kisa A, Kivimäki M, Koyanagi A, Krishnamurthi RK, Kumar GA, Lafranconi

A, Lewington S, Li S, Lo WD, Lopez AD, Lorkowski S, Lotufo PA, Mackay MT, Majdan M, Majdzadeh R, Majeed A, Malekzadeh R, Manafi N, Mansournia MA, Mehndiratta MM, Mehta V, Mengistu G, Meretoja A, Meretoja TJ, Miazgowski B, Miazgowski T, Miller TR, Mirrakhimov EM, Mohajer B, Mohammad Y, Mohammadoo-khorasani M, Mohammed S, Mohebi F, Mokdad AH, Mokhayeri Y, Moradi G, Morawska L, Moreno Velásquez I, Mousavi SM, Muhammed OSS, Muruet W, Naderi M, Naghavi M, Naik G, Nascimento BR, Negoi RI, Nguyen CT, Nguyen LH, Nirayo YL, Norrving B, Noubiap JJ, Ofori-Asenso R, Ogbo FA, Olagunju AT, Olagunju TO, Owolabi MO, Pandian JD, Patel S, Perico N, Piradov MA, Polinder S, Postma MJ, Poustchi H, Prakash V, Qorbani M, Rafiei A, Rahim F, Rahimi K, Rahimi-Movaghar V, Rahman M, Rahman MA, Reis C, Remuzzi G, Renzaho AMN, Ricci S, Roberts NLS, Robinson SR, Roever L, Roshandel G, Sabbagh P, Safari H, Safari S, Safiri S, Sahebkar A, Salehi Zahabi S, Samy AM, Santalucia P, Santos IS, Santos JV, Santric Milicevic MM, Sartorius B, Sawant AR, Schutte AE, Sepanlou SG, Shafieesabet A, Shaikh MA, Shams-Beyranvand M, Sheikh A, Sheth KN, Shibuya K, Shigematsu M, Shin M-J, Shiue I, Siabani S, Sobaih BH, Sposato LA, Sutradhar I, Sylaja PN, Szoeke CEI, Te Ao BJ, Temsah M-H, Temsah O, Thrift AG, Tonelli M, Topor-Madry R, Tran BX, Tran KB, Truelsen TC, Tsadik AG, Ullah I, Uthman OA, Vaduganathan M, Valdez PR, Vasankari TJ, Vasanthan R, Venketasubramanian N, Vosoughi K, Vu GT, Waheed Y, Weiderpass E, Weldegwergs KG, Westerman R, Wolfe CDA, Wondafrash DZ, Xu G, Yadollahpour A, Yamada T, Yatsuya H, Yimer EM, Yonemoto N, Yousefifard M, Yu C, Zaidi Z, Zamani M, Zarghi A, Zhang Y, Zodpey S, Feigin VL, Vos T, Murray CJL. Global, regional, and national burden of stroke, 1990–2016: a systematic analysis for the Global Burden of Disease Study 2016. *Lancet Neurol* 2019;**18**:439–458.

2. Campbell BCV, De Silva DA, Macleod MR, Coutts SB, Schwamm LH, Davis SM, Donnan GA. Ischaemic stroke. *Nat Rev Dis Primers* 2019;**5**:70.
3. Cheng YD, Al-Khoury L, Zivin JA. Neuroprotection for ischemic stroke: two decades of success and failure. *NeuroRx* 2004;**1**:36–45.
4. Saver JL, Starkman S, Eckstein M, Stratton SJ, Pratt FD, Hamilton S, Conwit R, Liebeskind DS, Sung G, Kramer I, Moreau G, Goldweber R, Sanossian N, Investigators F-M, Coordinators. Prehospital use of magnesium sulfate as neuroprotection in acute stroke. *N Engl J Med* 2015;**372**:528–536.
5. Savitz SI, Baron JC, Fisher M, Albers GW, Arbe-Barnes S, Boltze J, Broderick J, Broschat KO, Elkind MSV, En'Wezoh D, Furlan AJ, Gorelick PB, Grotta J, Hancock AM, Hess DC, Holt W, Houser G, Hsia AW, Kim W-K, Korinek WS, Le Moan N, Liberman M, Lilienfeld S, Luby M, Lynch JK, Mansi C, Simpkins AN, Nadareishvili Z, Nogueira RG, Pryor KE, Sanossian N, Schwamm LH, Selim M, Sheth KN, Spilker J, Solberg Y, Steinberg GK, Stice S, Tymianski M, Wechsler LR, Yoo AJ, Consortium SX. Stroke treatment academic industry roundtable X: brain cytoprotection therapies in the reperfusion era. *Stroke* 2019;**50**:1026–1031.
6. Matei N, Camara J, Zhang JH. The next step in the treatment of stroke. *Front Neurol* 2020;**11**:582605.
7. Hawkins BT, Davis TP. The blood-brain barrier/neurovascular unit in health and disease. *Pharmacol Rev* 2005;**57**:173–185.
8. Bell AH, Miller SL, Castillo-Melendez M, Malhotra A. The neurovascular unit: effects of brain insults during the perinatal period. *Front Neurosci* 2019;**13**:1452.
9. Kniesel U, Wolburg H. Tight junctions of the blood-brain barrier. *Cell Mol Neurobiol* 2000;**20**:57–76.
10. Kassner A, Merali Z. Assessment of blood-brain barrier disruption in stroke. *Stroke* 2015;**46**:3310–3315.
11. Planas AM. Role of immune cells migrating to the ischemic brain. *Stroke* 2018;**49**:2261–2267.
12. Yang C, Hawkins KE, Dore S, Candelario-Jalil E. Neuroinflammatory mechanisms of blood-brain barrier damage in ischemic stroke. *Am J Physiol Cell Physiol* 2019;**316**:C135–C153.
13. Bardutzky J, Schwab S. Antiedema therapy in ischemic stroke. *Stroke* 2007;**38**:3084–3094.
14. Andjelkovic AV, Xiang J, Stamatovic SM, Hua Y, Xi G, Wang MM, Keep RF. Endothelial targets in stroke: translating animal models to human. *Arterioscler Thromb Vasc Biol* 2019;**39**:2240–2247.
15. Cho S. CD36 as a therapeutic target for endothelial dysfunction in stroke. *Curr Pharm Des* 2012;**18**:3721–3730.
16. Kalluri AS, Vellarikkal SK, Edelman ER, Nguyen L, Subramanian A, Ellinor PT, Regev A, Kathiresan S, Gupta RM. Single-cell analysis of the normal mouse aorta reveals functionally distinct endothelial cell populations. *Circulation* 2019;**140**:147–163.
17. Febbraio M, Hajjar DP, Silverstein RL. CD36: a class B scavenger receptor involved in angiogenesis, atherosclerosis, inflammation, and lipid metabolism. *J Clin Invest* 2001;**108**:785–791.
18. Jimenez B, Volpert OV, Crawford SE, Febbraio M, Silverstein RL, Bouck N. Signals leading to apoptosis-dependent inhibition of neovascularization by thrombospondin-1. *Nat Med* 2000;**6**:41–48.
19. Moore KJ, El Khoury J, Medeiros LA, Terada K, Geula C, Luster AD, Freeman MW. A CD36-initiated signaling cascade mediates inflammatory effects of beta-amyloid. *J Biol Chem* 2002;**277**:47373–47379.
20. Chen K, Febbraio M, Li W, Silverstein RL. A specific CD36-dependent signaling pathway is required for platelet activation by oxidized low-density lipoprotein. *Circ Res* 2008;**102**:1512–1519.
21. Park L, Zhou J, Zhou P, Pistick R, El Jamal S, Younkin L, Pierce J, Arreguin A, Anrather J, Younkin SG, Carlson GA, McEwen BS, Iadecola C. Innate immunity receptor CD36 promotes cerebral amyloid angiopathy. *Proc Natl Acad Sci U S A* 2013;**110**:3089–3094.
22. Takahashi N, Kozai D, Kobayashi R, Ebert M, Mori Y. Roles of TRPM2 in oxidative stress. *Cell Calcium* 2011;**50**:279–287.
23. Fonfria E, Murdock PR, Cusdin FS, Benham CD, Kelsell RE, McNulty S. Tissue distribution profiles of the human TRPM cation channel family. *J Recept Signal Transduct Res* 2006;**26**:159–178.
24. Hecquet CM, Ahmmed GU, Vogel SM, Malik AB. Role of TRPM2 channel in mediating $H_2O_2$-induced $Ca^{2+}$ entry and endothelial hyperpermeability. *Circ Res* 2008;**102**:347–355.
25. Gelderblom M, Melzer N, Schattling B, Gob E, Hicking G, Arunachalam P, Bittner S, Ufer F, Herrmann AM, Bernreuther C, Glatzel M, Gerloff C, Kleinschnitz C, Meuth SG, Friese MA, Magnus T. Transient receptor potential melastatin subfamily member 2 cation channel regulates detrimental immune cell invasion in ischemic stroke. *Stroke* 2014;**45**:3395–3402.
26. Park L, Wang G, Moore J, Girouard H, Zhou P, Anrather J, Iadecola C. The key role of transient receptor potential melastatin-2 channels in amyloid-beta-induced neurovascular dysfunction. *Nat Commun* 2014;**5**:5318.
27. Mittal M, Nepal S, Tsukasaki Y, Hecquet CM, Soni D, Rehman J, Tiruppathi C, Malik AB. Neutrophil activation of endothelial cell-expressed TRPM2 mediates transendothelial neutrophil migration and vascular injury. *Circ Res* 2017;**121**:1081–1091.
28. Sommer CJ. Ischemic stroke: experimental models and reality. *Acta Neuropathol* 2017;**133**:245–261.
29. Mittal M, Urao N, Hecquet CM, Zhang M, Sudhahar V, Gao XP, Komarova Y, Ushio-Fukai M, Malik AB. Novel role of reactive oxygen species-activated trp melastatin channel-2 in mediating angiogenesis and postischemic neovascularization. *Arterioscler Thromb Vasc Biol* 2015;**35**:877–887.
30. Chen J, Wang L, Xu H, Xing L, Zhuang Z, Zheng Y, Li X, Wang C, Chen S, Guo Z, Liang Q, Wang Y. Meningeal lymphatics clear erythrocytes that arise from subarachnoid hemorrhage. *Nat Commun* 2020;**11**:3159.
31. Abdullahi W, Tripathi D, Ronaldson PT. Blood-brain barrier dysfunction in ischemic stroke: targeting tight junctions and transporters for vascular protection. *Am J Physiol Cell Physiol* 2018;**315**:C343–C356.
32. Posel C, Moller K, Boltze J, Wagner DC, Weise G. Isolation and flow cytometric analysis of immune cells from the ischemic mouse brain. *J Vis Exp* 2016;**53658**.
33. Lei TY, Ye YZ, Zhu XQ, Smerin D, Gu LJ, Xiong XX, Zhang HF, Jian ZH. The immune response of T cells and therapeutic targets related to regulating the levels of T helper cells after ischaemic stroke. *J Neuroinflammation* 2021;**18**:25.
34. Gan Y, Liu Q, Wu W, Yin JX, Bai XF, Shen R, Wang Y, Chen J, La Cava A, Poursine-Laurent J, Yokoyama W, Shi FD. Ischemic neurons recruit natural killer cells that accelerate brain infarction. *Proc Natl Acad Sci U S A* 2014;**111**:2704–2709.
35. Gelderblom M, Leypoldt F, Steinbach K, Behrens D, Choe CU, Siler DA, Arumugam TV, Orthey E, Gerloff C, Tolosa E, Magnus T. Temporal and spatial dynamics of cerebral immune cell accumulation in stroke. *Stroke* 2009;**40**:1849–1857.
36. Assmann JC, Muller K, Wenzel J, Walther T, Brands J, Thornton P, Allan SM, Schwaninger M. Isolation and cultivation of primary brain endothelial cells from adult mice. *Bio Protoc* 2017;**7**.
37. Tasca CI, Dal-Cim T, Cimarosti H. In vitro oxygen-glucose deprivation to study ischemic cell death. *Methods Mol Biol* 2015;**1254**:197–210.
38. Wang L, Geng J, Qu M, Yuan F, Wang Y, Pan J, Li Y, Ma Y, Zhou P, Zhang Z, Yang GY. Oligodendrocyte precursor cells transplantation protects blood-brain barrier in a mouse model of brain ischemia via Wnt/beta-catenin signaling. *Cell Death Dis* 2020;**11**:9.
39. Zong P, Feng J, Yue Z, Yu AS, Vacher J, Jellison ER, Miller B, Mori Y, Yue L. TRPM2 deficiency in mice protects against atherosclerosis by inhibiting TRPM2-CD36 inflammatory axis in macrophages. *Nat Cardiovasc Res* 2022;**1**:344–360.
40. Forstermann U, Munzel T. Endothelial nitric oxide synthase in vascular disease: from marvel to menace. *Circulation* 2006;**113**:1708–1714.
41. Atochin DN, Wang A, Liu VW, Critchlow JD, Dantas AP, Looft-Wilson R, Murata T, Salomone S, Shin HK, Ayata C, Moskowitz MA, Michel T, Sessa WC, Huang PL. The phosphorylation state of eNOS modulates vascular reactivity and outcome of cerebral ischemia in vivo. *J Clin Invest* 2007;**117**:1961–1967.
42. Forstermann U, Li H. Therapeutic effect of enhancing endothelial nitric oxide synthase (eNOS) expression and preventing eNOS uncoupling. *Br J Pharmacol* 2011;**164**:213–223.
43. Samdani AF, Dawson TM, Dawson VL. Nitric oxide synthase in models of focal ischemia. *Stroke* 1997;**28**:1283–1288.
44. Zong P, Feng J, Yue Z, Li Y, Wu G, Sun B, He Y, Miller B, Yu AS, Su Z, Xie J, Mori Y, Hao B, Yue L. Functional coupling of TRPM2 and extrasynaptic NMDARs exacerbates excitotoxicity in ischemic brain injury. *Neuron* 2022;**110**:1944–1958 e1948.
45. de la Monte SM, Jhaveri A, Maron BA, Wands JR. Nitric oxide synthase 3-mediated neurodegeneration after intracerebral gene delivery. *J Neuropathol Exp Neurol* 2007;**66**:272–283.
46. Yan J, Bengtson CP, Buchthal B, Hagenston AM, Bading H. Coupling of NMDA receptors and TRPM4 guides discovery of unconventional neuroprotectants. *Science* 2020;**370**.
47. Zorova LD, Popkov VA, Plotnikov EY, Silachev DN, Pevzner IB, Jankauskas SS, Babenko VA, Zorov SD, Balakireva AV, Juhaszova M, Sollott SJ, Zorov DB. Mitochondrial membrane potential. *Anal Biochem* 2018;**552**:50–59.
48. Baines CP, Kaiser RA, Purcell NH, Blair NS, Osinska H, Hambleton MA, Brunskill EW, Sayen MR, Gottlieb RA, Dorn GW, Robbins J, Molkentin JD. Loss of cyclophilin D reveals a critical role for mitochondrial permeability transition in cell death. *Nature* 2005;**434**:658–662.
49. Dugan LL, Sensi SL, Canzoniero LM, Handran SD, Rothman SM, Lin TS, Goldberg MP, Choi DW. Mitochondrial production of reactive oxygen species in cortical neurons following exposure to N-methyl-D-aspartate. *J Neurosci* 1995;**15**:6377–6388.
50. Murphy MP. How mitochondria produce reactive oxygen species. *Biochem J* 2009;**417**:1–13.
51. Loh KP, Ng G, Yu CY, Fhu CK, Yu D, Vennekens R, Nilius B, Soong TW, Liao P. TRPM4 inhibition promotes angiogenesis after ischemic stroke. *Pflugers Arch* 2014;**466**:563–576.
52. Balkaya M, Kim ID, Shakil F, Cho S. CD36 deficiency reduces chronic BBB dysfunction and scar formation and improves activity, hedonic and memory deficits in ischemic stroke. *J Cereb Blood Flow Metab* 2021;**41**:486–501.

53. Choi WS, Eom DS, Han BS, Kim WK, Han BH, Choi EJ, Oh TH, Markelonis GJ, Cho JW, Oh YJ. Phosphorylation of p38 MAPK induced by oxidative stress is linked to activation of both caspase-8- and -9-mediated apoptotic pathways in dopaminergic neurons. *J Biol Chem* 2004; **279**:20451–20460.
54. Chambers JW, LoGrasso PV. Mitochondrial c-Jun N-terminal kinase (JNK) signaling initiates physiological changes resulting in amplification of reactive oxygen species generation. *J Biol Chem* 2011;**286**:16052–16062.
55. Lin TN, Kim GM, Chen JJ, Cheung WM, He YY, Hsu CY. Differential regulation of thrombospondin-1 and thrombospondin-2 after focal cerebral ischemia/reperfusion. *Stroke* 2003;**34**:177–186.
56. Iruela-Arispe ML, Luque A, Lee N. Thrombospondin modules and angiogenesis. *Int J Biochem Cell Biol* 2004;**36**:1070–1078.
57. Lopez-Dee Z, Pidcock K, Gutierrez LS. Thrombospondin-1: multiple paths to inflammation. *Mediators Inflamm* 2011;**2011**:296069.
58. Zhang X, Kazerounian S, Duquette M, Perruzzi C, Nagy JA, Dvorak HF, Parangi S, Lawler J. Thrombospondin-1 modulates vascular endothelial growth factor activity at the receptor level. *FASEB J* 2009;**23**:3368–3376.
59. Du J, Xie J, Yue L. Intracellular calcium activates TRPM2 and its alternative spliced isoforms. *Proc Natl Acad Sci U S A* 2009;**106**:7239–7244.
60. Kraft R, Grimm C, Grosse K, Hoffmann A, Sauerbruch S, Kettenmann H, Schultz G, Harteneck C. Hydrogen peroxide and ADP-ribose induce TRPM2-mediated calcium influx and cation currents in microglia. *Am J Physiol Cell Physiol* 2004;**286**:C129–C137.
61. Tjalkens RB, Carbone DL, Wu G. Detection of nitric oxide formation in primary neural cells and tissues. *Methods Mol Biol* 2011;**758**:267–277.
62. Fernandez A, Meechan DW, Karpinski BA, Paronett EM, Bryan CA, Rutz HL, Radin EA, Lubin N, Bonner ER, Popratiloff A, Rothblat LA, Maynard TM, LaMantia AS. Mitochondrial dysfunction leads to cortical under-connectivity and cognitive impairment. *Neuron* 2019;**102**: 1127–1142 e1123.
63. Shimizu T, Dietz RM, Cruz-Torres I, Strnad F, Garske AK, Moreno M, Venna VR, Quillinan N, Herson PS. Extended therapeutic window of a novel peptide inhibitor of TRPM2 channels following focal cerebral ischemia. *Exp Neurol* 2016;**283**:151–156.
64. Cruz-Torres I, Backos DS, Herson PS. Characterization and optimization of the novel transient receptor potential melastatin 2 antagonist tatM2NX. *Mol Pharmacol* 2020;**97**:102–111.
65. Zhao Z, Nelson AR, Betsholtz C, Zlokovic BV. Establishment and dysfunction of the blood-brain barrier. *Cell* 2015;**163**:1064–1078.
66. Alim I, Teves L, Li R, Mori Y, Tymianski M. Modulation of NMDAR subunit expression by TRPM2 channels regulates neuronal vulnerability to ischemic cell death. *J Neurosci* 2013; **33**:17264–17277.
67. Huang J, Zhang R, Wang S, Zhang D, Leung CK, Yang G, Li Y, Liu L, Xu Y, Lin S, Wang C, Zeng X, Li J. Methamphetamine and HIV-Tat protein synergistically induce oxidative stress and blood-brain barrier damage via transient receptor potential melastatin 2 channel. *Front Pharmacol* 2021;**12**:619436.
68. Eroglu E, Saravi SSS, Sorrentino A, Steinhorn B, Michel T. Discordance between eNOS phosphorylation and activation revealed by multispectral imaging and chemogenetic methods. *Proc Natl Acad Sci U S A* 2019;**116**:20210–20217.
69. Suresh K, Servinsky L, Reyes J, Undem C, Zaldumbide J, Rentsendorj O, Modekurty S, Dodd OJ, Scott A, Pearse DB, Shimoda LA. CD36 mediates $H_2O_2$-induced calcium influx in lung microvascular endothelial cells. *Am J Physiol Lung Cell Mol Physiol* 2017;**312**:L143–L153.
70. Garcia-Bonilla L, Racchumi G, Murphy M, Anrather J, Iadecola C. Endothelial CD36 contributes to postischemic brain injury by promoting neutrophil activation via CSF3. *J Neurosci* 2015;**35**:14783–14793.
71. Chu LY, Ramakrishnan DP, Silverstein RL. Thrombospondin-1 modulates VEGF signaling via CD36 by recruiting SHP-1 to VEGFR2 complex in microvascular endothelial cells. *Blood* 2013;**122**:1822–1832.
72. Simard JM, Woo SK, Gerzanich V. Transient receptor potential melastatin 4 and cell death. *Pflugers Arch* 2012;**464**:573–582.
73. Woo SK, Kwon MS, Ivanov A, Gerzanich V, Simard JM. The sulfonylurea receptor 1 (Sur1)-transient receptor potential melastatin 4 (Trpm4) channel. *J Biol Chem* 2013;**288**: 3655–3667.
74. Mehta RI, Tosun C, Ivanova S, Tsymbalyuk N, Famakin BM, Kwon MS, Castellani RJ, Gerzanich V, Simard JM. Sur1-Trpm4 cation channel expression in human cerebral infarcts. *J Neuropathol Exp Neurol* 2015;**74**:835–849.
75. Autzen HE, Myasnikov AG, Campbell MG, Asarnow D, Julius D, Cheng Y. Structure of the human TRPM4 ion channel in a lipid nanodisc. *Science* 2018;**359**:228–232.
76. Sun Y, Vandenbriele C, Kauskot A, Verhamme P, Hoylaerts MF, Wright GJ. A human platelet receptor protein microarray identifies the high affinity immunoglobulin E receptor subunit alpha (FcepsilonR1alpha) as an activating platelet endothelium aggregation receptor 1 (PEAR1) ligand. *Mol Cell Proteomics* 2015;**14**:1265–1274.
77. Wang Y, Nakayama M, Pitulescu ME, Schmidt TS, Bochenek ML, Sakakibara A, Adams S, Davy A, Deutsch U, Luthi U, Barberis A, Benjamin LE, Makinen T, Nobes CD, Adams RH. Ephrin-B2 controls VEGF-induced angiogenesis and lymphangiogenesis. *Nature* 2010;**465**: 483–486.


## Translational perspective

- Endothelial-specific *Trpm2* deletion produces strong protective effects against ischemic stroke by preserving blood–brain barrier (BBB) integrity, inhibiting plasma extravasation, and inhibiting immune cell infiltration.
- Thrombospodin-1 (TSP1) activates endothelial TRPM2 in a CD36-dependent manner, leading to hyperpermeability of the BBB, therefore exacerbating ischemic stroke.
- TRPM2 activation is also required for CD36-induced endothelial dysfunction and subsequent tight junction degradation when exposed to oxygen–glucose deprivation (OGD) and TSP1.
- The TSP1–CD36–TRPM2 axis contributes to BBB degradation during ischemic stroke.
- Our data establish TRPM2 activation by TSP-1 as a new mechanism for endothelial hyperpermeability. Hence, TRPM2 in endothelial cells presents itself as a promising therapeutic target for mitigating BBB leakage during ischemic stroke.